23. Nakakuma H, Nagakura S, Iwamoto N, et al. Paroxysmal nocturnal hemoglobinuria clone in bone marrow of patients with pancytopenia. Blood. 1995;85:1371-1376.

24. Brodsky RA, Mukhina GL, Nelson KL, Lawrence TS, Jones RJ, Buckley JT. Resistance of paroxysmal nocturnal hemoglobinuria cells to the glycosylphosphatidylinositol-binding toxin aerolysin. Blood. 1999;93:1749-1756.

25. Agresti A. Analysis of Ordinal Categorical Data. New York, NY: John Wiley & Sons; 1984.

26. Maciejewski JP, Rivera C, Kook H, Dunn D, Young NS. Relationship between bone marrow failure syndromes and the presence of glycosphosphatidyl inositol-anchored protein-deficient clones. Br J Haematol. 2001;115:1015-1022.

27. Araten DJ, Bessler M, McKenzie S, et al. Dynamics of hematopoiesis in paroxysmal nocturnal hemoglobinuria (PNH): no evidence for intrinsic growth advantage of PNH clones. Leukemia. 2002;16:2243-2248.

28. Zeng W, Nakao S, Takamatsu H, et al. Characterization of T-cell repertoire of the bone marrow in immune-mediated aplastic anemia: evidence for the involvement of antigen-driven T-cell response in cyclosporine-dependent aplastic anemia. Blood. 1999;93:3006-3015.

29. Feng X, Chuhjo T, Sugimori C, et al. Diazepam-binding inhibitor-related protein 1: a candidate autoantigen in acquired aplastic anemia patients harboring a minor population of paroxysmal nocturnal hemoglobinuria-type cells. Blood. 2004; 104:2425-2431.

30. Takami A, Zeng W, Wang H, Matsuda T, Nakao S. Cytotoxicity against lymphoblastoid cells mediated by a T-cell clone from an aplastic anaemia patient: role of CD59 on target cells. Br J Haematol. 1999;107:791-796.

31. Murakami Y, Kosaka H, Maeda Y, et al. Inefficient response of T lymphocytes to glycosylphosphatidylinositol anchor-negative cells: implications for paroxysmal nocturnal hemoglobinuria. Blood. 2002;100:4116-4122.

32. Nagakura S, Ishihara S, Dunn DE, et al. Decreased susceptibility of leukemic cells with PIG-A mutation to natural killer cells in vitro. Blood. 2002;100:1031-1037.

33. McMahon EJ, Bailey SL, Castenada CV, Waldner H, Miller SD. Epitope spreading initiates in the CNS in two mouse models of multiple sclerosis. Nat Med. 2005;11:335-339.

STEM CELLS®
Original Article

# Two Different Roles of Purified CD45$^+$c-Kit$^+$Sca-1$^+$Lin$^-$ Cells After Transplantation in Muscles

MOMOKO YOSHIMOTO,[a] HSI CHANG,[a] MITSUTAKA SHIOTA,[a] HIROHIKO KOBAYASHI,[a] KATSUTSUGU UMEDA,[a] ATSUSHI KAWAKAMI,[b] TOSHIO HEIKE,[a] TATSUTOSHI NAKAHATA[a]

[a]Department of Pediatrics, Graduate School of Medicine, Kyoto University, Kyoto, Japan;
[b]Department of Biological Science, Graduate School of Sciences, University of Tokyo, Tokyo, Japan

**Key Words.** Hematopoietic stem cells • Transplantation • c-Kit$^+$Sca-1$^+$Lin$^-$ • Muscle stem cells

## ABSTRACT

**Recent studies have indicated that bone marrow cells can regenerate damaged muscles and that they can adopt phenotypes of other cells by cell fusion. Our direct visualization system gave evidence of massive muscle regeneration by green fluorescent protein (GFP)–labeled CD45$^+$c-Kit$^+$Sca-1$^+$Lin$^-$ cells (KSL cells), and we investigated the role of KSL cells in muscle regeneration after transplantation with or without lethal irradiation. In the early phase, GFP signals were clearly observed in all the muscles of only irradiated mice. Transverse cryostat sections showed GFP$^+$myosin$^+$ muscle fibers, along with numerous GFP$^+$ hematopoietic cells in damaged muscle. These phenomena were temporary, and GFP signals had dramatically reduced 30 days after transplantation. After 6 months, GFP$^+$ fibers could hardly be detected, but GFP$^+$c-Met$^+$ mononuclear cells were located beneath the basal lamina where satellite cells usually exist in both conditioned mice. Immunostaining of isolated single fibers revealed GFP$^+$PAX7$^+$, GFP$^+$MyoD$^+$, and GFP$^+$Myf5$^+$ satellite-like cells on the fibers. Single-fiber cultures from these mice showed proliferation of GFP$^+$ fibers. These results indicate two different roles of KSL cells: one leading to regeneration of damaged muscles in the early phase and the other to conversion into satellite cells in the late phase.** STEM CELLS *2005;23:610–618*

## INTRODUCTION

Various tissue-specific stem cells have been identified in epidermis [1], intestinal epithelium [2], testis [3], liver [4], brain [5], and muscle [6]. Until recently, it was thought that tissue-specific stem cells could only differentiate into their original tissue, but it has been demonstrated that they can also differentiate into other lineages. For example, cells of donor origin have been detected in liver, heart, vascular endothelium, skeletal muscles, and other organs after bone marrow (BM) transplantation [7–14]. Of special interest for our study is that BM-derived cells have been shown to participate in the regeneration of chemically damaged fibers in skeletal muscle [12]. Subsequent studies showed that dystrophin-positive myofibers were restored in mdx mice, an animal model of Duchenne's muscular dystrophy, after transplantation of stem cells purified by fluorescence-activated cell sorting with Hoechst 33342 low-stained cells, also known as side population (SP) cells [15]. In short, stem cells in BM, comprising hematopoietic stem cells (HSCs) and mesenchymal stem cells (MSCs), have been found to be capable of regenerating damaged muscle fibers after BM transplantation.

It has also been demonstrated, however, that BM cells can adopt the phenotype of other cells by means of cell fusion [16, 17]. These investigators warned that in vivo "transdifferentiation" might result from cell fusion. The differentiation potential of BM cells beyond the lineage restriction of stem cells remains to be determined.

Correspondence: Tatsutoshi Nakahata, M.D., Ph.D., Department of Pediatrics, Graduate School of Medicine, Kyoto University, 54 Kawahara-cho, Shogoin, Sakyo-ku, Kyoto 606-8507, Japan. Telephone: 81-75-751-3290; Fax: 81-75-752-2361; e-mail: tnakaha@kuhp.kyoto-u.ac.jp Received September 2, 2004; accepted for publication January 13, 2005.  1066-5099/2005/$12.00/0 doi: 10.1634/stemcells.2004-0220

In addition to BM cells, SP cells have also been identified in muscle tissues [15, 18]. These muscle SP cells are reported to have hematopoietic as well as myogenic potential [19] and to express CD45 antigen, which is recognized as a hematopoietic cell marker. Another study gave evidence that $CD45^+$ cells in skeletal muscle are of BM origin [20]. These reports thus indicate that hematopoietic cells of BM origin seem to be present in skeletal muscles. However, the correlations among HSCs, $CD45^+$ cells in skeletal muscle, satellite cells, myogenic precursors, and muscle-derived stem cells have not yet been determined. It is important to clarify these relationships, both for scientific research and for the application of stem cell therapy.

To investigate the potential and the kinetics of HSCs in skeletal muscles, we transplanted c-$Kit^+Sca\text{-}1^+Lin^-$ (KSL) cells as enriched HSC fraction from green fluorescent protein (GFP) transgenic mice into lethally irradiated C57BL/6 mice or nonirradiated $W/W^v$ neonates that can accept HSCs without myeloablation. We examined the time-course behavior of $GFP^+$ cells in recipient muscles with a fluorescent stereomicroscope and immunohistochemical staining during the early and late phases after transplantation. Our visualization system makes it possible to detect transplanted cells with GFP signals in intact organs without the need to make sections first and can easily trace their kinetics throughout the entire body [21]. With this system, we found that myeloablation enables KSL cells to migrate into damaged muscles and to regenerate muscle fibers in the whole body during the early phase following transplantation. In the late phase, progenies of KSL cells had remained in muscle tissues and gave rise to satellite cells with myogenic potential, regardless of whether the mice had been irradiated.

## Materials and Methods

### Mice

Pregnant female W/+ mice mated with $W^v$/+ mice were obtained from Shizuoka Laboratory Animal Center (Shizuoka, Japan). GFP transgenic mice were kindly provided by Dr. M. Okabe (Osaka University, Japan). The background of all these mice was C57BL/6. All cells except erythrocytes of transgenic mice expressed GFP protein. The mice were bred and maintained in a specific pathogen-free microisolator environment. Neomycin in acidic water was supplied to irradiated recipient adult mice during the first month after transplantation.

### Cell Sorting

BM cells were labeled with a cocktail of biotinated primary antibodies for CD3 (145-2C11), B220/CD45R (RA3-6B2), Mac-1 (M1/70), Gr-1 (RB6-8C5), and TER119 (TR119). All antibodies were purchased from Pharmingen (San Diego, http://www.bdbiosciences.com/pharmingen). Lineage-negative ($Lin^-$) cells were obtained by auto–magnetic cell sorting (MACS; Militenyi Biotec, Bergisch Gladbach, Germany, http://www.miltenyibiotec.com), according to the manufacturer's instructions. $Lin^-$ cells were then stained with phycoerythrin (PE)–conjugated anti-Sca-1 antibody and allophycocyanin (APC)–conjugated anti-c-Kit antibody. KSL cells were collected by cell sorting on a FACSVantage (Becton, Dickinson, San Jose, CA, http://www.bd.com). To confirm that KSL cells are all hematopoietic cells based on the expression of CD45 antigen, we stained $Lin^-$ cells collected from wild-type C57BL/6 mice with fluorescein isothiocyanate (FITC)–conjugated anti-CD45 antibody, PE-conjugated anti-Sca-1 antibody, and APC-conjugated anti-c-Kit antibody.

### Transplantation and Sequential Analysis

One to $5 \times 10^3$ of KSL cells with $2 \times 10^5$ Ly5.1 BM cells were injected into the tail vein of C57BL/6 adult mice that had received 9.0 Gy irradiation or into the orbital branch of the anterior facial vein of $W/W^v$ neonates within 0–3 days after birth. On days 3, 10, 20, and 30 after transplantation, all muscles were observed under a fluorescent stereomicroscope (Leica, Heerbrugg, Switzerland, http://www.leica.com). At least five mice were analyzed in each time point.

### Adherent Cell Culture

To see if KSL cells contain any mesenchymal cells, we cultured 1 to $5 \times 10^3$ per well of KSL cells with MesenCult Medium (Stem Cell Technologies, Vancouver, Canada, http://www.stemcell.com) in 24-well plates for 14 days.

### Immunohistochemistry

Muscles were fixed with 4% paraformaldehyde, embedded in the optimal cutting temperature compound. Frozen sections of 7-μm thickness were mounted on silane-coated glass slides. For immunostaining of single-muscle fiber [22], fibers were fixed with 4% paraformaldehyde and were permeabilized with 0.5% (vol/vol) Triton X-100 phosphate-buffered solution (PBS). Rabbit or mouse anti-GFP (BD Biosciences Clontech, Palo Alto, CA, http://www.bdbiosciences.com/clontech/), rat anti-CD45 (Pharmingen), mouse anti-myosin (Zymed Laboratories, San Francisco, http://www.zymed.com), mouse anti-myogenin, mouse anti-MyoD1 (Dako, Carpinteria, CA, http://www.ump.com/dako.html), rabbit anti-c-Met, rabbit anti-Myf5 (Santa Cruz Biotechnology, Santa Cruz, CA, http://www.scbt.com), rabbit anti-laminin (Dako), and mouse-anti PAX7 (generated from mouse hybridoma [23]) were used as the primary antibodies. Either alkaline phosphatase (ALP)–conjugated anti-rabbit, Alexa488-conjugated anti-rabbit, Alexa350-conjugated anti-rabbit, streptavisin Alexa350 Cy3–conjugated anti-rat or anti-mouse, FITC-conjugated anti-rabbit or anti-mouse was used as the secondary antibody. Hematoxylin or Hoechst 33324 was used for nuclear staining. These samples were then examined under a fluorescent microscope (Olympus, Tokyo, http://

www.olympus-global.com), an AS-MDW (Leica), or a confocal microscope (Olympus). Photographs were obtained with an AxioCam (Carl Zeiss Vision GmbH, Hallbergmoos, Germany, http://www.zeiss.com) or an AS-MDW (Leica).

### FISH Analysis

For the detection of GFP DNA in myonuclei of the tissues at 30 days and 6 months after transplantation, fluorescence in situ hybridization (FISH) analysis was done. GFP detection was made using a polymerase chain reaction (PCR) digoxigenin (DIG) probe synthesis kit (Roche, Basel, Switzerland, http://www.roche.com). Hybridization was done according to the instructions of in situ hybridization kit (Nippon Gene, Toyama, Japan, http://www.nippongene.jp). In brief, frozen sections were fixed in 100% ethanol, followed by incubation in 90%, 80%, 70%, and 50% ethanol. Sections were incubated in 50 μg/ml of proteinase K for 15 minutes at 37°C. The GFP probe was denatured at 95°C and added to each slide following incubation on a 95°C hotplate. The sections were hybridized overnight at 42°C in a humidified chamber. Sections were washed three times in 50% formamide in 2× sodium chloride/sodium citrate (SSC) prewarmed to 42°C, then in 0.1× SSC at 42°C. Sections were washed in PBS, and a hybridized GFP probe was detected using peroxidase-conjugated anti-DIG antibody (Dako), following tyramide signal amplification (PerkinElmer Life and Analytical Science, Inc., Boston, http://las.perkinelmer.com).

### Single-Fiber Culture

Single muscle fibers were explanted in matrigel-coated plates, as described previously [24]. Briefly, the bilateral soleus muscles were removed from the animal and incubated in collagenase for 90 minutes at 37°C. Digested fibers were then carefully explanted onto matrigel-coated 24-well plates. A plating medium, consisting of 10% horse serum (HS) and 0.5% chick embryo extract (Gibco, Carlsbad, CA, http://www.invitrogen.com) in Dulbecco's modified Eagle's medium (DMEM; Sigma Chemical Corp., St. Louis, http://www.sigma-aldrich.com) was added. The medium was replaced on day 4 with a growth medium consisting of 20% fetal calf serum (FCS), 10% HS, and 1% chick embryo extract in DMEM, and on day 8 with a differentiation medium, consisting of 2% FCS, 10% HS, and 0.5% chick embryo extract in DMEM.

### PCR Analysis

Total DNA was extracted with a Dneasy Tissue Kit (Qiagen, Valencia, CA, http://www1.qiagen.com) from the 24-well plates used for culturing single fibers from hind limb muscles 6 months after transplantation of KSL cells. The primers for GFP were (5'-3') CTG GTC GAG CTG GAC GGC GAC G and CAC GAA CTC CAG CAG GAC CAT G. For nested GFP they were ACA AGT TCA GCG TGT CCG GCG A and CTT CTC GTT GGG GTC TTT GCT C. The PCR cycle using AmpliTaq Gold (Applied Biosystems, Foster City, CA, http://www.appliedbiosystems.com) for the GFP or nested GFP primer comprised 8 minutes at 95°C, 35 cycles at 94°C for 30 seconds, at 64°C for 30 seconds, and at 72°C for 40 seconds, followed by 7 minutes at 72°C.

## Results

### KSL Cells Can Repair Muscle Damage in Early Phase After Transplantation

To investigate the process of settlement of donor hematopoietic cells into skeletal muscles, HSC fraction, KSL cells [25], derived from BM of GFP-transgenic mice, were transplanted into lethally irradiated adult mice by tail vein injection. The entire KSL cell fraction was hematopoietic and expressed CD45 (Fig. 1). The purity of KSL cells after sorting was 98%. To exclude the possibility of contamination of mesenchymal cells, we cultured 1 to 5 × $10^3$ per well of KSL cells with MesenCult medium for 14 days. No adherent cells were observed (data not shown).

After transplantation, the muscles in the entire body were examined, first with a fluorescent stereomicroscope and then with immunohistochemical staining, to detect the GFP signals. On day 3 after transplantation, no GFP signals could be detected in any muscles. On days 10 and 20, powerful GFP signals in

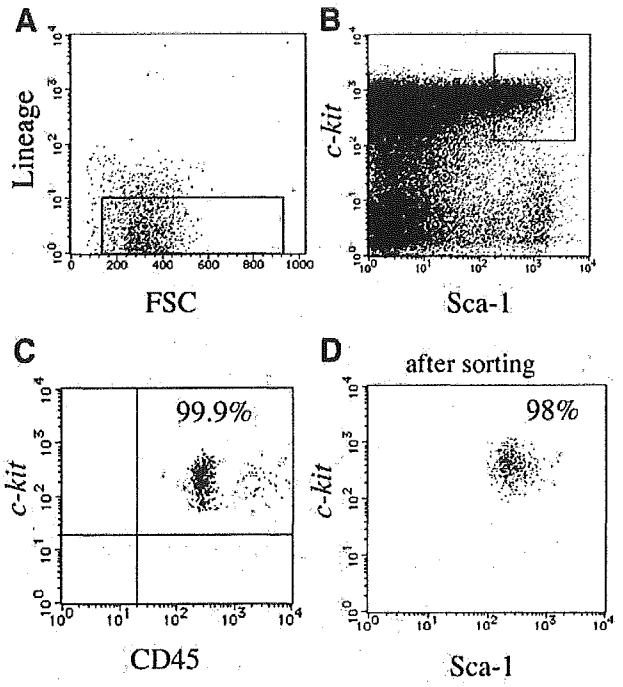


**Figure 1.** Purification of KSL cells. After collecting Lin⁻ cells by auto-MACS, KSL cells were sorted by FACSVantage. **(A):** Lin⁻ gating. **(B):** Sorting gate for KSL cells. **(C):** All KSL gated cells express CD45. **(D):** The purity of KSL cells after sorting was 98%. Abbreviation: FSC, forward scatter.

the muscle fibers throughout the body were observed under a fluorescent stereomicroscope such as in the intercostal, thigh, abdominal, greater pectoral, and external ocular muscles (Fig. 2A). Transverse sections showed muscle fibers of variable sizes with centrally localized nuclei, which represents the regenerative status (Fig. 2B). Among these muscle fibers, GFP$^+$ region–like muscle fibers were detected (Fig. 2B, b, arrowheads; faintly red region). There were mainly two types of GFP$^+$ regions. One region consisted of GFP$^+$ fibers (Fig. 3B), which were confirmed by typical cross-striations (Fig. 3A) and by immunostaining with anti-myosin antibody (Fig. 3C, D). And the other consisted of GFP$^+$ mononuclear cells (Fig. 3E), most of which were not stained with anti-myosin (Fig. 3G, H) but stained with anti-CD45 antibody (Fig. 3F, H). In the region of GFP$^+$ fibers, myogenin$^+$ myoblasts or myotubes were detected around the fibers (Fig. 4D, E, arrowheads). Interestingly, CD45$^{low}$myogenin$^+$GFP$^+$ cells were also detected (Fig. 4B–E, arrows) but only very few in number. This replacement by GFP$^+$ fibers could be observed only from day 10 to day 20 and had dramatically decreased on day 30 (Fig. 2A, g–i). FISH analysis revealed a small number of GFP-DNAs in myonuclei (data not shown). These results indicated that the irradiation for myeloablation evoked muscle injury and that KSL cells engrafted in damaged muscles, fusing the host's muscle fibers, and participated in muscle regeneration in the early phase of transplantation.

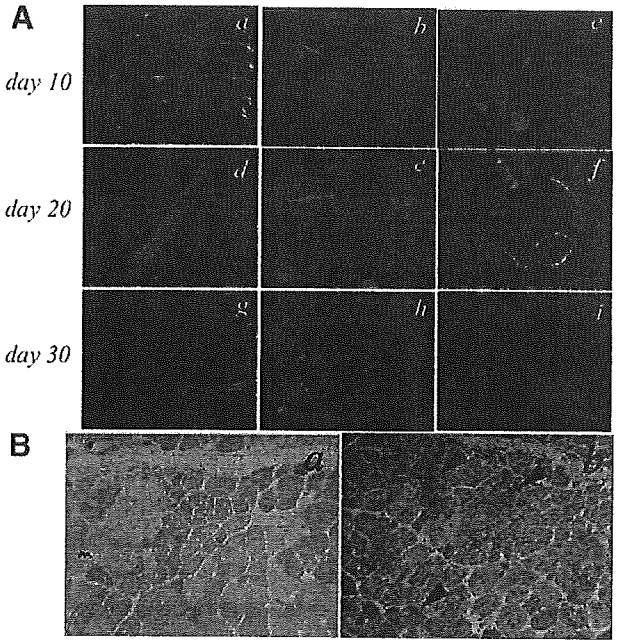


**Figure 2. (A):** Visualization of transplanted GFP$^+$ cells in muscles on days 10, 20, and 30. Appearances of various muscles under a fluorescent stereomicroscope are shown. Muscle tissues were removed from recipient mice and observed under a fluorescent stereomicroscope on days 10, 20, and 30 after transplantation. a, d, g: Intercostal muscle (the white lines indicate the shape of ribs). b: Abdominal muscle. c: Thigh muscle. e: Greater pectoral muscle. f: External ocular muscle (the white line indicates the shape of the eyeball). h: Dorsal muscle. Bars: a–c, e, 2 mm; d, 500 μm; f–g, i, 1 mm; h, 200 μm. **(B):** Immunohistostaining of the section of muscle tissues on day 10. a: Negative control. b: The section was stained with anti-GFP antibodies (alkaline phosphatase, faintly red region; arrowheads), and hematoxylin was used for nuclear staining.

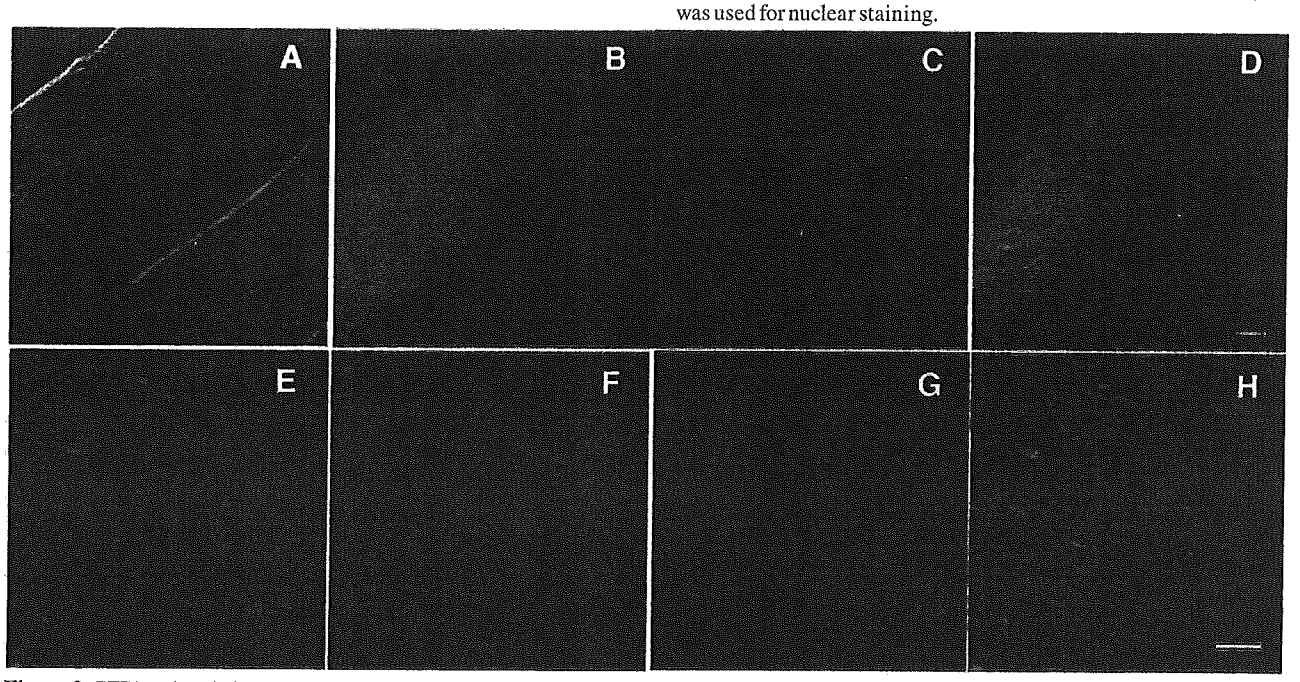


**Figure 3.** GFP$^+$ regions in intercostal muscle on day 20. Intercostal muscles were removed from recipient mice and fixed with 4% paraformaldehyde and made into frozen sections, as described in Materials and Methods. There were two types of GFP regions: **(A–D)** GFP$^+$ fibers and **(E–H)** GFP$^+$ mononuclear cells. Each section was stained with anti-GFP antibody (**B, D, E, H**, green), anti-myosin antibody (**C, D**, Cy3 red; **G, H**, Alexa350 blue), and anti-CD45 antibody (**F, H**, Cy3 red). **(A):** Phase contrast **(D, H):** Merge. Bars: D, 10 μm; H, 20 μm.

### KSL Cells Settle in Muscle Tissue Like a Satellite Cell

Sections of the muscle tissues obtained 30 days and 6 months after transplantation were stained with anti-GFP and anti-laminin (a marker of the basal lamina) antibodies, showing that several GFP$^+$ cells were located inside the basal lamina with laminin expression (Fig. 5A), which is where satellite cells are usually found. GFP$^+$ cells under the basal lamina were coexpressed with c-Met antigen (a marker of satellite cells) (Fig. 5E, arrows). Furthermore, we isolated single fibers from soleus muscles 2 months after transplantation and stained them with anti-PAX7, MyoD, or Myf5, which are specific satellite cell markers. We detected Myf5$^+$GFP$^+$ satellite cells on the fibers (Fig. 6A–D), but neither PAX7$^+$GFP$^+$ cells nor MyoD$^+$GFP$^+$ cells (data not shown). These results suggested that GFP$^+$ KSL cells migrate into muscle tissues, with some of them localizing beneath the basal lamina expressing satellite cell markers.

### KSL Cells Can Settle in Muscle Tissues Without Muscle Damage

Tissue-specific stem cells occupy niches—microenvironments that maintain self-renewal activity and multipotency of stem cells. Since it is known that irradiation depletes endogenous satellite cells and that injected muscle precursors can replace them [26], we used lethal irradiation for the transplantation assay. However, lethal irradiation also evokes various responses in the body. To exclude the influence of irradiation damage, we next transplanted KSL cells into W/W$^v$ neonates. W/W$^v$ mice possess a c-Kit gene mutation and can accept transplanted HSCs in a BM niche without irradiation [27]. Moreover, transplantation into W/W$^v$ neonates results in a higher chimeric ratio than does transplantation into adults [28]. Our experiments using transplantation into W/W$^v$ neonates showed no evidence of GFP$^+$ muscle fibers at any time, whereas BM cells were almost entirely replaced. However, small GFP$^+$ mononuclear cells could be detected between muscle fibers as early as 30 days after transplantation (Fig. 7A). Some GFP$^+$ cells were also detected beneath the laminin-positive basement

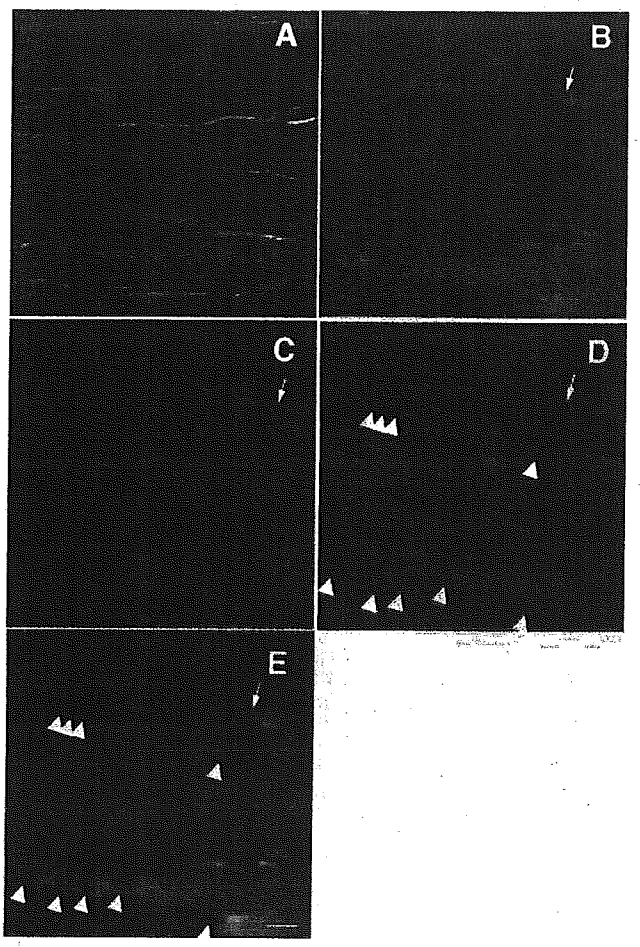


**Figure 4.** Myogenic phenotype of a CD45$^+$ cell in muscle tissues on day 20. **(A, B):** GFP$^+$ muscle structure showed cross striations. These sections were stained with anti-CD45 antibody (**C**, Cy3 red) and anti-myogenin antibody (**D**, blue). **(E):** Merge. Myogenin$^+$ myoblast- or myotube-like cells were detected (**D, E,** arrowhead), and an elongated GFP$^+$ cell coexpressed myogenin and CD45 (**B–E,** arrow).

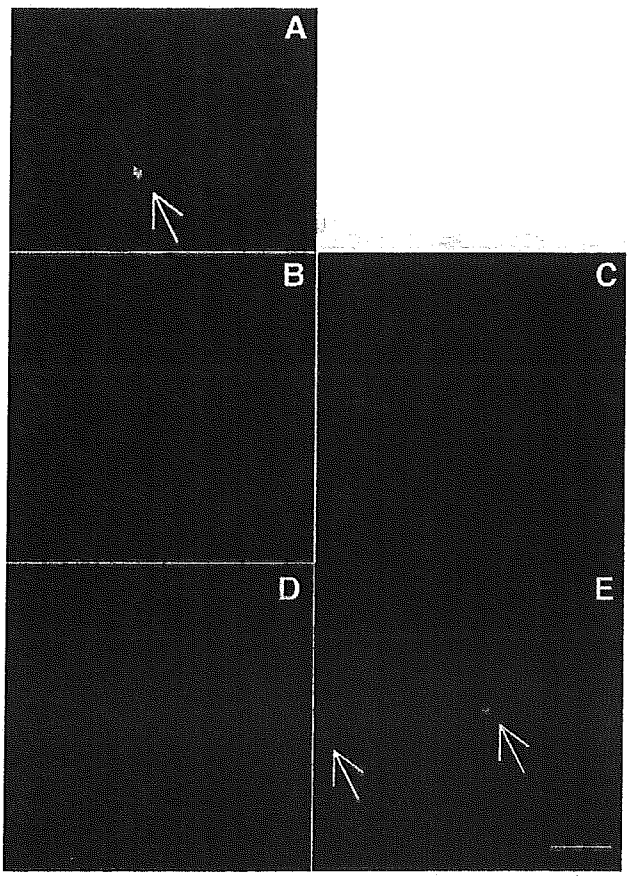


**Figure 5.** GFP$^+$ cells localized like satellite cells long term after transplantation. Sections from 6 months after transplantation were stained with laminin (**A**, Cy3 red; **D, E,** Alexa350 blue) and c-Met (**C, E,** Cy3 red) GFP$^+$ cells localized under the basal lamina (**A, E,** arrows) and were costained with c-Met (**E,** arrows). Bar: 20 μm.

membrane (Fig. 7B), and some of them were also stained with anti-c-Met antibody (Fig. 7C). We also examined isolated single fibers 1 month after transplantation and detected MyoD$^+$GFP$^+$ cells and PAX7$^+$GFP$^+$ cells on the fibers (Fig. 6H, L). We could also detect Myf5$^+$GFP$^+$ cells on the fibers 2 months after transplantation (Fig. 6P). These results showed that KSL cells and/or their progenies could migrate into undamaged muscle tissues expressing satellite cell–specific markers also, and that a suitable microenvironment for them might exist in skeletal muscles.

### KSL-Derived Cells in Muscle Can Generate Muscle Fibers In Vitro in Long Term After Transplantation

So far it has been reported that damaged muscles by chemical agent or stress were regenerated by donor cells after BM transplantation [12, 15]. However, these muscle-regeneration assays in vivo cannot clarify whether donor cells participate in regenerating muscles directly from the settled muscle or indirectly from settled BM. To determine whether GFP$^+$ mononuclear cells in muscle tissues can differentiate into muscle fibers, a single-fiber culture was performed. Six months after transplantation with KSL cells,

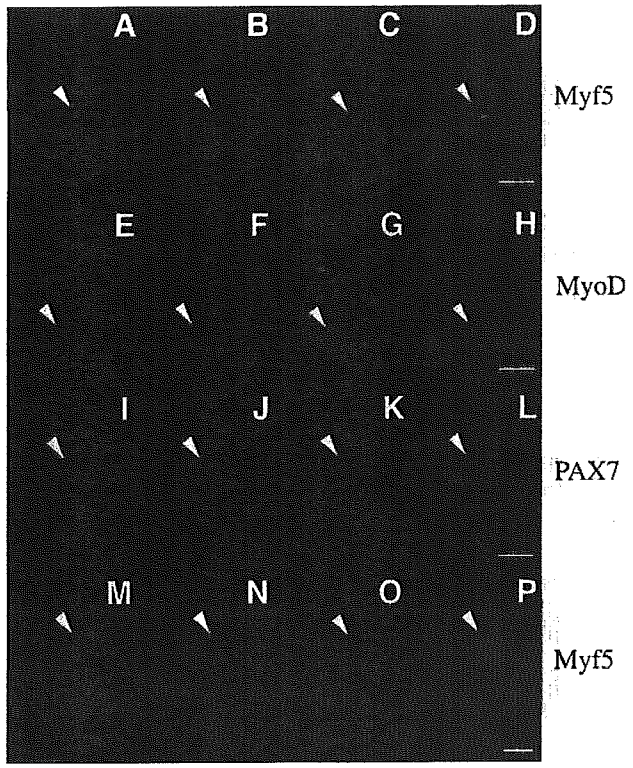


**Figure 6.** Immunostaining of single fibers. Single fibers were isolated from **(A–D)** irradiated mice 2 months after transplantation and from **(E–P)** W/W$^v$ mice 1 or 2 months after transplantation and were stained with satellite cell–specific markers. **(A, E, I, M):** Anti-GFP antibody (FITC green, arrowheads). **(B, N):** Anti-Myf5 antibody (Cy3 red, arrowheads). **(F):** Anti-MyoD1 antibody (Cy3 red, arrowhead). **(J):** Anti-PAX7 antibody (Cy3 red, arrowhead). **(D, H, L, P):** Merge. Bars: D, P, 50 μm; H, L, 100 μm.

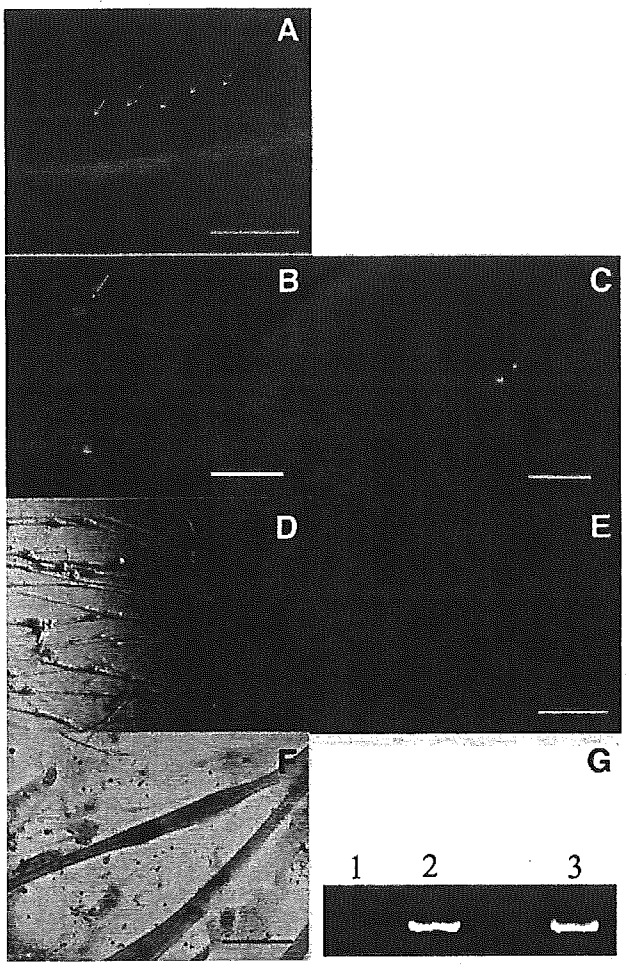


**Figure 7.** Analysis of the potential of GFP$^+$ satellite-like cells in muscle 6 months after transplantation. Thirty days and 6 months after nonirradiated transplantation into W/W$^v$ neonates, GFP$^+$ mononuclear cells were detected between muscle fibers under fluorescent stereomicroscope (**A**, arrows). In the sections, immunostaining for laminin and c-Met was performed (**B, C**). **(A):** Appearance of rib and rib muscle under fluorescent stereomicroscope on day 30. Some GFP$^+$ mononuclear cells were detected (arrows). The white lines indicate the shape of ribs. **(B):** Immunohistochemistry with anti-laminin (Cy3 red) and anti-GFP antibodies. A confocal microscope was used to determine the precise location of GFP$^+$ cells. GFP$^+$ cells beneath basal lamina (arrow) were detected on day 30 and 6 months later. **(C):** GFP$^+$ cell under laminin-positive basal lamina (Alexa350 blue) was also stained with anti c-Met antibody (Cy3 red, arrow). **(D–F):** Single-fiber culture was performed with single fibers isolated from recipient mice 6 months after transplantation, followed by immunostaining. C, negative control; D, anti-myosin (Cy3 red) staining; E, anti-GFP-ALP (red) staining. D and E were same position. GFP-ALP$^+$ fibers were confirmed to be muscle fibers using myosin Cy3 staining. **(G):** PCR analysis of extracted DNA from single-fiber culture. DNA was extracted from the single-fiber culture followed by PCR for GFP DNA, as described under Materials and Methods. 1: negative control; 2: peripheral blood of GFP transgenic mouse; 3: single fiber culture. Bars: A, 1 mm; B, C, 20 μm; D, 200 μm; E, F, 50 μm.

muscle fibers were isolated from the hind limb muscles of W/W$^v$ mice or lethally irradiated mice transplanted, and single fibers were cultured onto matrigel-coated plates. After 14 days, most of the satellite cells had migrated from the fibers, proliferated, and formed new muscle fibers, which were confirmed to be myosin-positive by immunohistochemical staining (Fig. 7D, E). Since the GFP signal in vitro was too weak to be detected by fluorescent microscope, we determined the presence of GFP$^+$ cells by means of immunohistochemical staining using the anti-GFP antibody or by GFP DNA amplification with the aid of PCR. Staining with the anti-GFP antibody proved the presence of GFP$^+$ myofibers (Fig. 7F), which were also myosin-positive. In addition, GFP DNA was also confirmed by PCR to be present in samples extracted from culture dishes of single-muscle fiber (Fig. 7G). No GFP$^+$ fibers were generated in the single-fiber culture in the early phase of transplantation in irradiated mice (data not shown). In brief, GFP$^+$ KSL cell that engrafted muscle tissues could repair damaged muscle but not produce muscle fibers in vitro in the early phase. In the long term, however, they acquired the potential to differentiate into muscle fibers like satellite cells also in vitro. Since the single-fiber culture is a functional assay of the presence of satellite cells, it can be said that GFP$^+$ KSL cells can give rise to satellite cells with myogenic potential in the long term after transplantation.

## Discussion

In this study, we showed early repair of damaged muscles by KSL cells and first demonstrated that KSL cells could differentiate into satellite-like cells in skeletal muscle in the long term after transplantation (Fig. 8).

The thoroughly studied and identified characteristics of surface markers for HSCs showed that our KSL cells contained a dominant stem cell population. A single CD34$^{-/low}$ c-Kit$^+$Sca-1$^+$ Lin$^-$ cell (CD34$^-$ KSL cell) has been demonstrated to be capable of reconstituting long-term hematopoiesis in about 30% of lethally irradiated adult mice [25]. Our $1 \times 10^3$ of KSL cells contained about 5%–10% of CD34$^-$ cells, which was enough to reconstitute BM of the irradiated mice, and hardly any CD45$^-$ cells (less than 0.1%; Fig. 1). And we cultured 1 to $5 \times 10^3$ of KSL cells for 14 days and obtained no adherent cells. It can therefore be safely assumed that the $1 \times 10^3$ of KSL cells were originally all hematopoietic and did not contain any mescenchymal cells, which do not express CD45 antigen, demonstrating that CD45$^+$ KSL cells can differentiate into muscle fibers. So far, unfractionated BM cells have been used to demonstrate transdifferentiation to muscle fibers [12, 29]. LaBarge and Blau [30] reported recently on the biological progression from adult BM cells to muscle stem cells to muscle fiber, and their findings support our hypothesis. Their study used unfractionated BM cells, which contained both HSCs and MSCs. In contrast, we used CD45$^+$ KSL cells as the enriched HSC fraction, and we showed that KSL cells could contribute to muscle regeneration in both the early and late phases after transplantation. Very recently, it has been reported that a single HSC generated skeletal muscle [31, 32]. These reports support our results. BM SP cells are the same as HSCs and are reported to be involved in muscle regeneration after transplantation, but no satellite cells derived from BM SP cells have been documented [15, 31]. Our study, by analyzing single fibers, is the first to demonstrate that CD45$^+$ KSL cells can give rise to satellite cells both in vivo and in vitro. Since BM SP cells and KSL cells are still heterogeneous populations, further classification of HSCs may lead to the identification of a subpopulation specific to muscle regeneration.

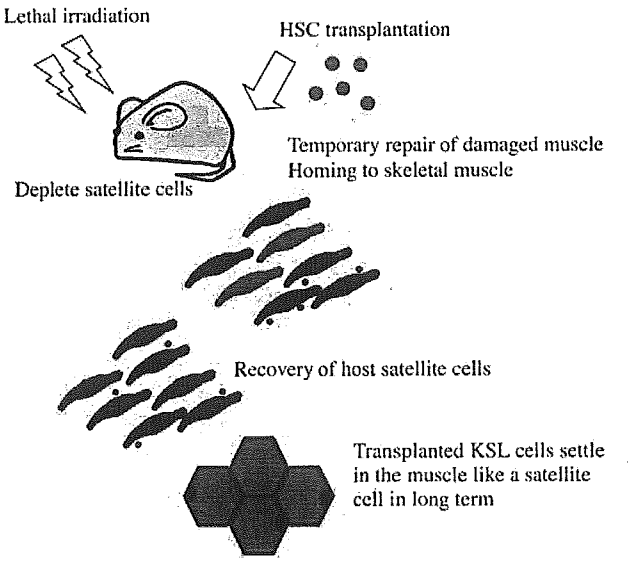


**Figure 8.** Schematic representation of hypothesized behavior of transplanted KSL cells in muscle tissues. See Discussion for a detailed explanation. Abbreviation: HSC, hematopoietic stem cell.

It has been reported that mononuclear cells harvested from murine skeletal muscle are capable of hematopoietic reconstitution in lethally irradiated mice and that these muscle-derived hematopoietic progenitor cells are originally derived from BM [20, 33]. However, determination of the time when these hematopoietic cells settle in muscles after transplantation, as well as the histological identification of their location in muscle tissues, has not yet been accomplished. Our observations demonstrate that GFP$^+$ mononuclear cells gather in damaged muscles before BM has been fully replaced. Nearly all of these GFP$^+$ mononuclear cells consist of CD45$^+$ in muscle fibers. Interestingly, a few CD45$^{low}$myogenin$^+$GFP$^+$ cells were also detected, and this implies that transplanted KSL cells might have an important and direct role in regeneration in the very early phase after transplantation.

Thirty days after transplantation, single fibers from irradiated mice were not stained by anti-PAX7, anti-MyoD, or anti-Myf5 antibody, and they did not grow in vitro in culture, whereas myofibers could develop in vitro in single-fiber culture from age-matched nontreated mice. Because it is said that irradiation eliminates satellite cells [26, 34], these phenomena might mean that satellite cells had been damaged by irradiation at this

time point. We speculated that, after 30 days, host satellite cells recovered from radiation damage, producing new muscle fibers, which replaced GFP+ fibers gradually. We assume that GFP+ fibers were diluted, fusing with host-derived muscle fibers. Simultaneously, GFP+ cells remain beneath the basal lamina as satellite cells in muscle tissue and acquire the potential to differentiate into muscle fibers in the long term after transplantation. In this late phase, muscle regeneration can be obtained from GFP+ satellite-like cells, as well as from endogenous satellite cells, as was confirmed by single-fiber culture. We therefore propose two different roles of KSL cells in muscle regeneration: repair of muscles damaged by irradiation in the early phase, and generating satellite cells in the late phase.

In the case of transplantation into W/W$^v$ neonates, GFP+ cells engrafted into muscle tissues as early as 30 days after transplantation without irradiation. Interestingly, we could detect satellite cell markers MyoD, PAX7, and Myf5 on GFP+ cells on muscle fibers as early as 1 or 2 months after transplantation. GFP+ single fibers can develop in vitro at the same time (data not shown). This means that KSL cells can migrate into muscle fibers and become satellite-like cells without muscle damage. We therefore speculate that KSL cells might be part of a physiological satellite cell source. Neonatal environment might give some effect to KSL cells. And it is not yet clear why hematopoietic cells engraft into undamaged muscles. The fact that CD45+ hematopoietic cells engraft into skeletal muscles suggests the existence of some muscle-specific molecular mechanism for HSC engraftment. During the processes of HSC homing and engraftment into BM, the contribution of some adhesion molecules such as VCAM-1, which is a ligand for α4 integrins, has been reported [35, 36]. HSCs are reported to have α4 integrins [37]. Furthermore, laminin, which is a ligand for α4 integrin, which in turn is a component of muscle basement membrane, may be important for the maintenance of hematopoietic cells in skeletal muscles.

About 1,000 KSL cells, which proved to be enough to reconstitute BM of irradiated mice, are also sufficient to distribute throughout all the muscles in the body and regenerate all damaged muscles such as intercostals, diaphragm, and limb muscles. This is an important finding in terms of potential for clinical application. Patients with muscular dystrophy suffer from respiratory distress due to respiratory muscle weakness. Our findings of powerful engraftment of transplanted KSL cells in the entire body, including respiratory muscles, may be the first step on the way to the establishment of therapeutic strategies using HSCs. Further studies are needed, however, to establish efficient engraftment of HSCs to muscle tissues and to identify responsible molecules.

## Acknowledgments

This study was supported by Health and Labour Science Research Grant, Research on Human Genome, Tissue Engineering Food Biotechnology, Ministry of Health, Labour and Welfare, Tokyo; by Grant-in-Aid for Science Research on Priority Areas no. 122150-67; and by Grant-in-Aid for Creative Scientific Research no. 13GS-0009. This study was also supported by Research Grant no. 13B-1 for Nervous and Mental Disorders and no. H13-iyaku-043, both from the Ministry of Health, Labour and Welfare.

## References

1 Taylor G, Lehrer MS, Jensen PJ et al. Involvement of follicular stem cells in forming not only the follicle but also the epidermis. Cell 2000;102:451–461.

2 Mills JC, Gordon JI. The intestinal stem cell niche: there grows the neighborhood. Proc Natl Acad Sci U S A 2001;98:12334–12336.

3 Shinohara T, Orwig KE, Avarbock MR et al. Remodeling of the postnatal mouse testis is accompanied by dramatic changes in stem cell number and niche accessibility. Proc Natl Acad Sci U S A 2001;98:6186–6191.

4 Suzuki A, Zheng Yw YW, Kaneko S et al. Clonal identification and characterization of self-renewing pluripotent stem cells in the developing liver. J Cell Biol 2002;156:173–184.

5 Rietze RL, Valcanis H, Brooker GF et al. Purification of a pluripotent neural stem cell from the adult mouse brain. Nature 2001;412:736–739.

6 Qu-Petersen Z, Deasy B, Jankowski R et al. Identification of a novel population of muscle stem cells in mice: potential for muscle regeneration. J Cell Biol 2002;157:851–864.

7 Petersen BE, Bowen WC, Patrene KD et al. Bone marrow as a potential source of hepatic oval cells. Science 1999;284:1168–1170.

8 Orlic D, Kajstura J, Chimenti S et al. Bone marrow cells regenerate infarcted myocardium. Nature 2001;410:701–705.

9 Brazelton TR, Rossi FM, Keshet GI et al. From marrow to brain: expression of neuronal phenotypes in adult mice. Science 2000;290:1775–1779.

10 Mezey E, Chandross KJ, Harta G et al. Turning blood into brain: cells bearing neuronal antigens generated in vivo from bone marrow. Science 2000;290:1779–1782.

11 Lagasse E, Connors H, Al-Dhalimy M et al. Purified hematopoietic stem cells can differentiate into hepatocytes in vivo. Nat Med 2000;6:1229–1234.

12 Ferrari G, Cusella-De Angelis G, Coletta M et al. Muscle regeneration by bone marrow-derived myogenic progenitors. Science 1998;279:1528–1530.

13 Bittner RE, Schofer C, Weipoltshammer K et al. Recruitment of bone-marrow-derived cells by skeletal and cardiac muscle in adult dystrophic mdx mice. Anat Embryol (Berl) 1999;199:391–396.

14 Krause DS, Theise ND, Collector MI et al. Multi-organ, multi-lineage engraftment by a single bone marrow-derived stem cell. Cell 2001;105:369–377.

15 Gussoni E, Soneoka Y, Strickland CD et al. Dystrophin expression in the mdx mouse restored by stem cell transplantation. Nature 1999;401:390–394.

16 Terada N, Hamazaki T, Oka M et al. Bone marrow cells adopt the phenotype of other cells by spontaneous cell fusion. Nature 2002;416:542–545.

17 Ying QL, Nichols J, Evans EP et al. Changing potency by spontaneous fusion. Nature 2002;416:545–548.

18 Jackson KA, Mi T, Goodell MA. Hematopoietic potential of stem cells isolated from murine skeletal muscle. Proc Natl Acad Sci U S A 1999;96:14482–14486.

19 Asakura A, Seale P, Girgis-Gabardo A et al. Myogenic specification of side population cells in skeletal muscle. J Cell Biol 2002;159:123–134.

20 Kawada H, Ogawa M. Bone marrow origin of hematopoietic progenitors and stem cells in murine muscle. Blood 2001;98:2008–2013.

21 Yoshimoto M, Shinohara T, Heike T et al. Direct visualization of reconstitution process of transplanted hematopoietic cells in intact mouse organs indicates the presence of a niche. Exp Hematol 2003;31:733–740.

22 Zammit PS, Golding JP, Nagata Y et al. Muscle satellite cells adopt divergent fates: a mechanism for self-renewal? J Cell Biol 2004;166:347–357.

23 Kawakami A, Kimura-Kawakami M, Nomura T et al. Distributions of PAX6 and PAX7 proteins suggest their involvement in both early and late phases of chick brain development. Mech Dev 1997;66:119–130.

24 Rosenblatt JD, Lunt AI, Parry DJ et al. Culturing satellite cells from living single muscle fiber explants. In Vitro Cell Dev Biol Anim 1995;31:773–779.

25 Osawa M, Hanada K, Hamada H et al. Long-term lymphohematopoietic reconstitution by a single CD34–low/negative hematopoietic stem cell. Science 1996;273:242–245.

26 Blaveri K, Heslop L, Yu DS et al. Patterns of repair of dystrophic mouse muscle: studies on isolated fibers. Dev Dyn 1999;216:244–256.

27 Mintz B, Anthony K, Litwin S. Monoclonal derivation of mouse myeloid and lymphoid lineages from totipotent hematopoietic stem cells experimentally engrafted in fetal hosts. Proc Natl Acad Sci U S A 1984;81:7835–7839.

28 Capel B, Mintz B. Neonatal W-mutant mice are favorable hosts for tracking development of marked hematopoietic stem cells. Exp Hematol 1989;17:872–876.

29 Fukada S, Miyagoe-Suzuki Y, Tsukihara H et al. Muscle regeneration by reconstitution with bone marrow or fetal liver cells from green fluorescent protein-gene transgenic mice. J Cell Sci 2002;115:1285–1293.

30 LaBarge MA, Blau HM. Biological progression from adult bone marrow to mononucleate muscle stem cell to multinucleate muscle fiber in response to injury. Cell 2002;111:589–601.

31 Camargo FD, Green R, Capetenaki Y et al. Single hematopoietic stem cells generate skeletal muscle through myeloid intermediates. Nat Med 2003;9:1520–1527.

32 Corbel SY, Lee A, Yi L et al. Contribution of hematopoietic stem cells to skeletal muscle. Nat Med 2003;9:1528–1532.

33 McKinney-Freeman SL, Jackson KA, Camargo FD et al. Muscle-derived hematopoietic stem cells are hematopoietic in origin. Proc Natl Acad Sci U S A 2002;99:1341–1346.

34 Heslop L, Morgan JE, Partridge TA. Evidence for a myogenic stem cell that is exhausted in dystrophic muscle. J Cell Sci 2000;113(Pt 12):2299–2308.

35 Schweitzer KM, Drager AM, van der Valk P et al. Constitutive expression of E-selectin and vascular cell adhesion molecule-1 on endothelial cells of hematopoietic tissues. Am J Pathol 1996;148:165–175.

36 Jacobsen K, Kravitz J, Kincade PW et al. Adhesion receptors on bone marrow stromal cells: in vivo expression of vascular cell adhesion molecule-1 by reticular cells and sinusoidal endothelium in normal and gamma-irradiated mice. Blood 1996;87:73–82.

37 Williams DA, Rios M, Stephens C et al. Fibronectin and VLA-4 in haematopoietic stem cell-microenvironment interactions. Nature 1991;352:438–441.

# Development of functional human blood and immune systems in NOD/SCID/IL2 receptor γ chain$^{null}$ mice

Fumihiko Ishikawa, Masaki Yasukawa, Bonnie Lyons, Shuro Yoshida, Toshihiro Miyamoto, Goichi Yoshimoto, Takeshi Watanabe, Koichi Akashi, Leonard D. Shultz, and Mine Harada

**Here we report that a new nonobese diabetic/severe combined immunodeficient (NOD/SCID) mouse line harboring a complete null mutation of the common cytokine receptor γ chain (NOD/SCID/interleukin 2 receptor [IL2r] γ$^{null}$) efficiently supports development of functional human hemato-lymphopoiesis. Purified human (h) CD34$^+$ or hCD34$^+$hCD38$^-$ cord blood (CB) cells were transplanted into NOD/SCID/IL2rγ$^{null}$ newborns via a facial vein. In all recipients injected with $10^5$ hCD34$^+$ or $2 \times 10^4$ hCD34$^+$hCD38$^-$ CB cells, human hematopoietic cells were reconstituted at approximately 70% of chimerisms. A high percentage of the human hematopoietic cell chimerism persisted for more than 24 weeks after transplantation, and hCD34$^+$ bone marrow grafts of primary recipients could reconstitute hematopoiesis in secondary NOD/SCID/IL2rγ$^{null}$ recipients, suggesting that this system can support self-renewal of human hematopoietic stem cells. hCD34$^+$hCD38$^-$ CB cells differentiated into mature blood cells, including myelomonocytes, dendritic cells, erythrocytes, platelets, and lymphocytes. Differentiation into each lineage occurred via developmental intermediates such as common lymphoid progenitors and common myeloid progenitors, recapitulating the steady-state human hematopoiesis. B cells underwent normal class switching, and produced antigen-specific immunoglobulins (Igs). T cells displayed the human leukocyte antigen (HLA)–dependent cytotoxic function. Furthermore, human IgA-secreting B cells were found in the intestinal mucosa, suggesting reconstitution of human mucosal immunity. Thus, the NOD/SCID/IL2rγ$^{null}$ newborn system might be an important experimental model to study the human hemato-lymphoid system. (Blood. 2005;106:1565-1573)**



## Introduction

To analyze human immune and hematopoietic development and function in vivo, a number of studies have been tried to reproduce human hematopoiesis in small animal xenotransplantation models.[1] Successful transplantation of human hematopoietic tissues in immune-compromised mice was first reported in late 1980s by using homozygous severe combined immunodeficient (C.B.17-SCID) mice. In the first model of a humanized lymphoid system in a SCID mouse (SCID-hu model), McCune et al simultaneously transplanted human fetal tissues, including fetal liver hematopoietic cells, thymus, and lymph nodes, into SCID mice and induced mature human T- and B-cell development.[2] Mosier et al successfully reconstituted human T and B cells by transferring human blood mononuclear cells into SCID mice.[3] These initial studies suggested the usefulness of immunodeficient mice for reconstitution of the human lymphoid system from human bone marrow hematopoietic stem cells (HSCs).

After these initial reports, a number of modified SCID models have been proposed to try to reconstitute human immunity.[4] In addition, recombination activating gene (RAG)–deficient strains have been used as recipients in xenotransplantation: T- and B-cell–deficient *Prkdc*$^{scid}$, *Rag1*$^{-/-}$, or *Rag2*$^{-/-}$ mutant mice[5-7] were capable of supporting engraftment of human cells. The engraftment levels in these models, however, were still low, presumably due to the remaining innate immunity of host animals.[1] Nonobese diabetic/severe combined immunodeficient (NOD/SCID) mice have been shown to support higher levels of human progenitor cell engraftment than BALB/c/SCID or C.B.17/SCID mice.[8] Levels of human cell engraftment were further improved by treating NOD/SCID mice with anti-asialo GM1 (ganglioside-monosialic acid) antibodies[9] that can abrogate natural killer (NK) cell activity. Recently, NOD/SCID mice harboring either a null allele at the $\beta_2$-microglobulin gene (NOD/SCID/β2m$^{-/-}$)[10] or a truncated common cytokine receptor γ chain (γc) mutant lacking its cytoplasmic region (NOD/SCID/γc$^{-/-}$)[11,12] were developed. In these mice, NK- as well as T- and B-cell development and functions are disrupted, because β2m is necessary for major histocompatibility complex (MHC) class I–mediated innate immunity, and because γc (originally called IL-2Rγ chain) is an indispensable component

From the Department of Medicine and Biosystemic Science, Kyushu University Graduate School of Medical Sciences, Fukuoka, Japan; First Department of Internal Medicine, Ehime University School of Medicine, Shigenobu, Japan; The Jackson Laboratory, Bar Harbor, ME; Center for Cellular and Molecular Medicine, Kyushu University Hospital, Fukuoka, Japan; RIKEN for Allergy and Immunology, Yokohama, Japan; and the Department of Cancer Immunology and AIDS, Dana-Farber Cancer Institute, Boston, MA.

Submitted February 9, 2005; accepted April 7, 2005. Prepublished online as *Blood* First Edition Paper, May 26, 2005; DOI 10.1182/blood-2005-02-0516.

Supported by grants from Japan Society for Promotion of Science (F.I.); the Ministry of Education, Culture, Sports, Science and Technology of Japan (M.Y.); the Ministry of Health, Labor, and Welfare of Japan (M.H.); and National Institutes of Health grants A130389 and HL077642 (L.D.S.) and DK061320 (K.A.).

The online version of the article contains a data supplement.

**Reprints:** Koichi Akashi, Department of Cancer Immunology and AIDS, Dana-Farber Cancer Institute, 44 Binney St, no. 770, Boston, MA 02115; e-mail: koichi_akashi@dfci.harvard.edu; or Leonard D. Shultz, The Jackson Laboratory, 600 Main St, Bar Harbor, ME 04609.

The publication costs of this article were defrayed in part by page charge payment. Therefore, and solely to indicate this fact, this article is hereby marked "advertisement" in accordance with 18 U.S.C. section 1734.

of receptor heterodimers for many lymphoid-related cytokines (ie, IL-2, IL-7, IL-9, IL-12, IL-15, and IL-21).[13] Injection of human bone marrow or cord blood (CB) cells into these mice resulted in successful generation of human T and B cells. In our hands, efficiencies of CB cell engraftment represented by percentages of circulating human (h) CD45$^+$ cells were significantly (2- to 5-fold) higher in NOD/SCID/$\beta$2m$^{-/-}$ newborns than those in adults (F.I., M.H., and L.D.S., unpublished data, April 2003). More recently, transplantation of hCD34$^+$ CB cells into Rag2$^{-/-}$ $\gamma$c$^{-/-}$ newborns regenerated adaptive immunity mediated by functional T and B cells,[14] suggesting heightened support for xenogeneic transplants especially in the neonatal period. Efficiency of reconstitution of human hematopoiesis may be, however, still suboptimal in these models because chimerisms of human cells are not stable in each experiment.[11,12,14] Furthermore, there is little information regarding reconstitution of human myeloerythroid components in these xenogeneic models.

Two types of mouse lines with truncated or complete null $\gamma$c mutant[15-17] have been reported. NOD/SCID/$\gamma_c^{-/-}$ and Rag2$^{-/-}$ $\gamma$c$^{-/-}$ mouse strains harbor a truncated $\gamma$c mutant lacking the intracellular domain,[15] and therefore, binding of $\gamma$c-related cytokines to each receptor should normally occur in these models.[18] For example, IL-2R with the null $\gamma$c mutations would be an $\alpha\beta$ heterodimer complex with an affinity approximately 10 times lower than that of the high affinity $\alpha\beta$-$\gamma$ heterotrimer complex in mice with the truncated $\gamma$c mutant.[19] $\gamma$c has also been shown to dramatically increase the affinity to its ligands through the receptors for IL-4, IL-7, and IL-15.[20-23] Previous studies suggested that $\gamma$c-related receptors including IL-2R$\beta$ chain and IL-4R$\alpha$ chain could activate janus-activated kinases (JAKs) to some extent in the presence of the extracellular domain of $\gamma$c, independent of the cytoplasmic domain of $\gamma$c.[24,25] Thus, in order to block the signaling through $\gamma$c-related cytokine receptors more completely, we made NOD/SCID mice harboring complete null mutation of $\gamma$c[16] (the NOD/SCID/IL2r$\gamma^{null}$ strain). By using NOD/SCID/IL2r$\gamma^{null}$ newborns, we successfully reconstituted myeloerythroid as well as lymphoid maturation by injecting human CB or highly-enriched CB HSCs at a high efficiency. Reconstitution of human hematopoiesis persisted for a long term. The developing lymphoid cells were functional for immunoglobulin (Ig) production and human leukocyte antigen (HLA)–dependent cytotoxic activity. Our data show that the NOD/SCID/IL2r$\gamma^{null}$ newborn system provides a valuable tool to reproduce human hemato-lymphoid development.

## Materials and methods

### Mice

NOD.Cg-*Prkdc*$^{scid}$*IL2rg*$^{tm1Wjl}$/Sz (NOD/SCID/IL2r$\gamma^{null}$) and NOD/LtSz-*Prkdc*$^{scid}$/*B2m*$^{null}$ (NOD/SCID/$\beta$2m$^{null}$) mice were developed at the Jackson Laboratory (Bar Harbor, ME). The NOD/SCID/IL2r$\gamma^{null}$ strain was established by backcrossing a complete null mutation at $\gamma$c locus[16] onto the NOD.Cg-*Prkdc*$^{scid}$ strain. The establishment of this mouse line has been reported elsewhere.[26] All experiments were performed according to the guideline in the Institutional Animal Committee of Kyushu University.

### Cell preparation and transplantation

CB cells were obtained from Fukuoka Red Cross Blood Center (Japan). CB cells were harvested after written informed consent. Mononuclear cells were depleted of Lin$^+$ cells using mouse anti-hCD3, anti-hCD4, anti-hCD8, anti-hCD11b, anti-hCD19, anti-hCD20, anti-hCD56, and anti–human glycophorin A (hGPA) monoclonal antibodies (BD Immunocytometry, San Jose, CA). Samples were enriched for hCD34$^+$ cells by using anti-hCD34 microbeads (Miltenyi Biotec, Auburn, CA). These cells were further stained with anti-hCD34 and hCD38 antibodies (BD Immunocytometry), and were purified for Lin$^-$CD34$^+$CD38$^-$ HSCs by a FACSVantage (Becton Dickinson, San Jose, CA). Lin$^-$ hCD34$^+$ cells ($10^5$) or $2 \times 10^4$ Lin$^-$hCD34$^+$hCD38$^-$ cells were transplanted into irradiated (100 cGy) NOD/SCID/IL2r$\gamma^{null}$ or NOD/SCID/$\beta$2m$^{null}$ newborns via a facial vein[27] within 48 hours of birth.

### Examination of hematopoietic chimerism

At 3 months after transplantation, samples of peripheral blood, bone marrow, spleen, and thymus were harvested from recipient mice. Human common lymphoid progenitors were analyzed based on the expression of hCD127 (IL-7 receptor $\alpha$ chain) and hCD10 in Lin$^-$ (hCD3, hCD4, hCD8, hCD11b, hCD19, hCD20, hCD56, and hGPA)$^-$ hCD34$^+$hCD38$^-$ fraction.[28,29] Human myeloid progenitors were analyzed based on the expressions of hCD45RA and hCD123 (IL-3 receptor $\alpha$ chain) in Lin$^-$ CD10$^-$CD34$^+$CD38$^+$ fractions. For the analysis of megakaryocyte/erythroid (MegE) lineages, anti-hCD41a (HIP8), anti-hGPA (GAR-2), anti-mCD41a (MW Reg30), and anti-mTer119 (Ter-119) antibodies were used. Samples were treated with ammonium chloride to eliminate mature erythrocytes, and were analyzed by setting nucleated cell scatter gates. For the analysis of circulating erythrocytes and platelets, untreated blood samples were analyzed by setting scatter gates specific for each cell fraction. Human B lymphoid progenitors were evaluated according to the criteria proposed by LeBien.[30]

### Methylcellulose culture assay

Bone marrow cells of recipient mice were stained with anti-hCD34, hCD38, hCD45RO, hCD123, and lineage antibodies. Human HSCs, CMPs, GMPs, and MEPs were purified according to the phenotypic definition[28,29] by using a FACSVantage (Becton Dickinson). One hundred cells of each population were cultured in methylcellulose media (Stem Cell Technologies, Vancouver, BC, Canada) supplemented with 10% bovine serum albumin (BSA), 20 $\mu$g/mL steel factor, 20 ng/mL IL-3, 20 ng/mL IL-11, 20 ng/mL Fms-like tyrosine kinase 3 (Flt3) ligand, 50 ng/mL granulocyte-macrophage colony-stimulating factor (GM-CSF), 4 U/ml erythropoietin (Epo), and 50 ng/mL thrombopoietin (Tpo). Colony numbers were enumerated on day 14 of culture.

### Histologic analysis

Tissue samples were fixed with 4% paraformaldehyde and dehydrated with graded alcohol. After treatment with heated citrate buffer for antigen retrieval, paraformaldehyde-fixed paraffin-embedded sections were immunostained with mouse anti-hCD19, anti–human IgA, anti-hCD3, anti-hCD4, anti-hCD8, and anti-hCD11c antibodies (Dako Cytomation, Carpinteria, CA). Stained specimens were observed by confocal microscopy (LSM510 META microscope; Carl Zeiss, Oberkochen, Germany). Image acquisition and data analysis were performed by using LSM5 software. Numerical aperture of the objective lens (PlanApochromat ×63) used was 1.4.

### ELISA

Human Ig concentration in recipient sera was measured by using a human immunoglobulin assay kit (Bethyl, Montgomery, IL). For detection of ovalbumin (OVA)–specific human IgM and IgG antibodies, 5 recipient mice were immunized twice every 2 weeks with 100 $\mu$g of OVA (Sigma, St Louis, MO) that were emulsified in aluminum hydroxide (Sigma). Sera from OVA-treated mice were harvested 2 weeks after the second immunization. OVA was plated at s concentration of 20 $\mu$g/mL on 96-microtiter wells at 4°C overnight. After washing and blocking with bovine serum albumin, serum samples were incubated in the plate for 1 hour. Antibodies binding OVA were then measured by a standard enzyme-linked immunosorbent assay (ELISA).

### Cytotoxicity of alloantigen-specific human CD4+ and CD8+ T-cell lines

Alloantigen-specific human CD4+ and CD8+ T-cell lines were established according to the method as reported.[31] After stimulation with an Epstein Barr virus–transformed B lymphoblastoid cell line (TAK-LCL) established from a healthy individual (TAK-LCL) for 6 days, 100 hCD4+ T cells or hCD8+ T cells were plated with $3 \times 10^4$ TAK-LCL cells in the presence of 10 U/mL human IL-2 (Genzyme, Boston, MA), and were subjected to a chromium 51 ($^{51}Cr$) release assay. A Limiting number of effector cells and $10^4$ $^{51}Cr$-labeled allogeneic target cells were incubated. KIN-LCLs that do not share HLA with effector cells or TAK-LCL were used as negative controls. Cytotoxic activity was tested in the presence or absence of anti-HLA class I or anti–HLA-DR monoclonal antibodies.

## Results

### Reconstitution of human hematopoiesis is achieved in NOD/SCID/IL2rγ$^{null}$ mice

NOD/SCID/IL2rγ$^{null}$ mice lacked mature murine T or B cells evaluated by fluorescence-activated cell sorting (FACS), and displayed extremely low levels of NK cell activity.[31] This mouse line can survive more than 15 months[31] since it does not develop thymic lymphoma, usually a fatal disease in the immune-compromised mice with NOD background.[32]

Lin−hCD34+ CB cells contain HSCs, and myeloid and lymphoid progenitors.[28,29] We and others have reported that engraftment of human CB cells, which contain hematopoietic stem and progenitor cells, was efficient in NOD/SCID/β2m$^{-/-}$ and RAG2$^{-/-}$/γc$^{-/-}$ mice, especially when cells were transplanted during the neonatal period.[14,33] We therefore transplanted purified Lin−hCD34+ CB cells into sublethally irradiated NOD/SCID/IL2rγ$^{null}$ newborns via a facial vein.[27]

We first transplanted $10^5$ Lin−hCD34+ CB cells from 3 independent donors into 5 NOD/SCID/IL2rγ$^{null}$ newborns, and found that the NOD/SCID/IL2rγ$^{null}$ newborn system is very efficient for supporting engraftment of human hematopoietic progenitor cells. Table 1 shows percentages of hCD45 cells in these mice 3 months after transplantation. Strikingly, the average engraftment levels were approximately 70% in both the bone marrow and the peripheral blood. Compared with 4 control NOD/SCID/β2m$^{-/-}$ recipient mice given transplants from the same donors, engraftment levels of hCD45+ cells in NOD/SCID/IL2rγ$^{null}$ mice were significantly higher (Table 1).

Table 1. Chimerism of human CD45+ cells in NOD/SCID/β2m$^{null}$ mice and NOD/SCID/IL2rγ$^{null}$ mice

| Mouse no. (donor no.) | % nucleated cells | | |
|---|---|---|---|
| | PB | BM | Spleen |
| NOD/SCID/IL2rγ$^{null}$ | | | |
| 1 (1) | 71.2 | 70.9 | 66.8 |
| 2 (1) | 81.7 | 81.4 | 47.1 |
| 3 (2) | 50.1 | 58.8 | 49.5 |
| 4 (3) | 68.0 | 83.1 | 51.1 |
| 5 (3) | 73.3 | 70.1 | 58.1 |
| Mean ± SD | 68.9 ± 11.6* | 72.9 ± 9.8* | 54.5 ± 8.0* |
| NOD/SCID/β2m$^{null}$ | | | |
| 1 (1) | 10.4 | 46.1 | 22.0 |
| 2 (2) | 11.6 | 31.5 | 24.3 |
| 3 (3) | 6.9 | 18.1 | 20.7 |
| 4 (3) | 20.7 | 30.4 | 31.2 |
| Mean ± SD | 12.4 ± 5.9* | 31.5 ± 11.5* | 22.6 ± 4.7* |

To compare the engraftment levels in the two strains, $1 \times 10^5$ Lin− CD34+ cells derived from 3 CB samples were transplanted into 5 NOD/SCID/IL2rγ$^{null}$ mice and 4 NOD/SCID/β2m$^{null}$ mice. At 3 months after transplantation, BM, spleen, and peripheral blood (PB) of the recipient mice were analyzed for the engraftment of human cells. Data show percentages of human CD45+ cells in each tissue.

*$P < .05$.

Table 2 shows the analysis of human hematopoietic cell progeny in mice that received transplants of human Lin−hCD34+ CB cells. In the peripheral blood, hCD45+ cells included hCD33+ myeloid, hCD19+ B cells, and hCD3+ T cells in all mice analyzed (Figure 1A and Table 2). We then analyzed the reconstitution of erythropoiesis and thrombopoiesis in these mice. Anti–human glycophorin A (hGPA) antibodies recognized human erythrocytes, while mTer119 antibodies[34] recognized GPA-associated protein on murine erythrocytes, respectively (Figure 1B). Human and murine platelets could also be stained with anti–human and anti–murine CD41a, respectively (Figure 1B). Circulating hGPA+ erythrocytes and hCD41a+ platelets were detected in all 3 mice analyzed (Figure 1B, right panels). hGPA+ erythroblasts and hCD41a+ megakaryocytes were detected as 9.5% ± 6.2% (n = 5) and 1.64% ± 0.42% (n = 5) of nucleated bone marrow cells, respectively. Thus, transplanted human Lin−hCD34+ CB cells differentiated into mature erythrocytes and platelets in NOD/SCID/IL2rγ$^{null}$ recipients.

In all engrafted mice, the bone marrow and the spleen contained significant numbers of hCD11c+ dendritic cells as well as hCD33+ myeloid cells, hCD19+ B cells, and hCD3+ T cells (Table 2 and Figure 1C). hCD11c+ dendritic cells coexpressed HLA-DR that is essential for antigen presentation to T cells (Figure 1D). In contrast, in the thymus, the majority of cells were composed of hCD3+ T cells and rare hCD19+ B cells (Table 2).

Figure 2A shows the change in the percentage of circulating hCD45+ cells in another set of NOD/SCID/IL2rγ$^{null}$ newborns injected with $2 \times 10^4$ Lin−hCD34+hCD38− CB cells. Surprisingly, the level of hCD45+ cells in the blood was unchanged, and was maintained at a high level even 24 weeks after transplantation. Mice did not develop lymphoid malignancies or other complications. Furthermore, we tested the retransplantability of human HSCs in primary recipients. We killed mice at 24 weeks after the primary transplantation of hCD34− cells, purified 1 to $5 \times 10^4$ hCD34+ cells from primary recipient bone marrow cells, and retransplanted them into NOD/SCID/IL2rγ$^{null}$ newborns. In all 3 experiments, secondary recipients successfully reconstituted human hematopoiesis at least until 12 weeks after transplantation, when we killed mice for the bone marrow analysis (Figure 2B). Thus, the NOD/SCID/IL2rγ$^{null}$ newborn system can support human hematopoiesis for the long term.

### Human cord blood hematopoietic stem cells produced myeloid and lymphoid cells via developmental intermediates in the NOD/SCID/IL2rγ$^{null}$ bone marrow

The Lin−hCD34+ CB fraction contains early myeloid and lymphoid progenitors as well as HSCs.[28] To verify that differentiation into all hematopoietic cells can be initiated from human HSCs in the NOD/SCID/IL2rγ$^{null}$ newborn system, we transplanted Lin−hCD34+hCD38− CB cells that contain the counterpart population of murine long-term HSCs,[35] and are highly enriched for human HSCs.[36,37] hCD34+ CB cells (15%-20%) were hCD38− (data not shown). Mice given transplants of $2 \times 10^4$ Lin−hCD34+hCD38− cells displayed successful reconstitution of similar proportion of human cells compared with mice reconstituted with $1 \times 10^5$ Lin−hCD34+ cells at 12 weeks after transplantation (Table 2). In another experiment, mice injected with $2 \times 10^4$ Lin−hCD34+hCD38− cells exhibited the high chimerism (> 50%)

Table 2. Cellular number and composition in tissues of engrafted NOD/SCID/IL2rγ$^{null}$ mice

| Injected cells, mice, and tissue type | Total no. cells | % nucleated cells (% hCD45$^+$ cells) | | | |
|---|---|---|---|---|---|
| | | CD33 | CD19 | CD3 | CD11c |
| 1 × 10$^5$ Lin$^-$CD34$^+$ | | | | | |
| Mouse no. 1/ donor no. 1 | | | | | |
| BM | 2.4 × 10$^7$ | 8.2 (11.6) | 54.8 (77.6) | 10.7 (15.1) | 1.1 (1.6) |
| Spleen | 4.1 × 10$^7$ | 4.3 (6.4) | 33.5 (50.1) | 26.1 (39.1) | 2.2 (3.3) |
| Thymus | 3.1 × 10$^5$ | NE | 1.3 (1.3) | 96.2 (98.7) | NE |
| PB | NE | 4.0 (5.6) | 35.1 (49.3) | 19.8 (27.8) | NE |
| Mouse no. 2/donor no. 1 | | | | | |
| BM | 1.8 × 10$^7$ | 5.5 (6.8) | 56.5 (67.6) | 9.9 (12.2) | 2.9 (3.6) |
| Spleen | 3.2 × 10$^7$ | 2.1 (4.5) | 27.7 (58.8) | 15.9 (33.8) | 1.3 (2.8) |
| Thymus | 4.5 × 10$^5$ | NE | 1.1 (1.2) | 90.4 (98.8) | NE |
| PB | NE | 6.1 (7.5) | 53.8 (65.9) | 21.6 (40.1) | NE |
| Mouse no. 4/ donor no. 3 | | | | | |
| BM | 1.9 × 10$^7$ | 9.4 (11.3) | 52.9 (63.7) | 15.9 (19.1) | 0.62 (0.75) |
| Spleen | 4.4 × 10$^7$ | 3.5 (6.8) | 24.2 (47.4) | 20.8 (40.7) | 1.5 (2.9) |
| Thymus | 0.8 × 10$^5$ | NE | 0.88 (1.1) | 78.2 (98.9) | NE |
| PB | NE | 3.2 (4.7) | 61.3 (90.1) | 5.3 (7.8) | NE |
| Mouse no. 5/donor no. 3 | | | | | |
| BM | 2.1 × 10$^7$ | 10.2 (14.6) | 48.8 (82.0) | 9.4 (13.4) | 1.3 (1.9) |
| Spleen | 2.7 × 10$^7$ | 6.6 (11.4) | 30.4 (52.3) | 18.6 (32.0) | 1.1 (1.9) |
| Thymus | 1.1 × 10$^5$ | NE | 3.1 (3.7) | 81.1 (96.3) | NE |
| PB | NE | 9.8 (13.4) | 40.4 (55.1) | 16.8 (22.9) | NE |
| 2 × 10$^4$ Lin$^-$CD34$^+$CD38$^-$ | | | | | |
| Mouse no. 6/donor no. 4 | | | | | |
| BM | 2.6 × 10$^7$ | 3.1 (5.3) | 46.1 (78.7) | 8.1 (13.8) | 1.3 (2.2) |
| Spleen | 3.9v10$^7$ | 1.3 (2.7) | 40.2 (83.9) | 5.9 (12.3) | 0.54 (1.1) |
| Thymus | 1.9 × 10$^5$ | NE | 2.1 (2.3) | 89.4 (97.7) | NE |
| PB | NE | 5.4 (12.4) | 28.9 (66.3) | 9.3 (21.3) | NE |
| Mouse no. 7/donor no. 5 | | | | | |
| BM | 1.4 × 10$^7$ | 7.2 (14.2) | 39.6 (78.1) | 3.1 (6.1) | 0.82 (1.6) |
| Spleen | 2.2 × 10$^7$ | 2.4 (5.1) | 37.2 (79.3) | 6.8 (14.5) | 0.52 (1.1) |
| Thymus | 1.3 × 10$^5$ | NE | 0.6 (0.7) | 85.1 (99.2) | NE |
| PB | NE | 2.3 (41.7) | 49.3 (89.5) | 3.5 (6.4) | NE |
| Mouse no. 8/donor no. 6 | | | | | |
| BM | 1.1 × 10$^7$ | 6.1 (11.7) | 36.8 (70.6) | 7.7 (14.8) | 2.5 (4.8) |
| Spleen | 2.9 × 10$^7$ | 2.9 (4.6) | 33.8 (53.1) | 24.6 (38.6) | 2.4 (3.8) |
| Thymus | 1.9 × 10$^5$ | NE | 1.1 (1.2) | 94.1 (97.0) | NE |
| PB | NE | 8.1 (11.9) | 50.2 (73.5) | 10.0 (14.6) | NE |

BM, spleen, and thymus were harvested from engrafted NOD/SCID/IL2rγ$^{null}$ mice at 3 months after transplantation. Total cell numbers in BM and thymus represent the cells harvested from 2 femurs for BM and those harvested from a hemilobe for thymus. Recipients 1, 2, 4, and 5 received transplants of 1 × 10$^5$ Lin$^-$CD34$^+$ cells. Recipients 6, 7, and 8 received transplants of 2 × 10$^4$ Lin$^-$CD34$^+$CD38$^-$ cells. NE indicates not examined.

of circulating human blood cells even 24 weeks after transplantation (not shown), suggesting the long-term engraftment of self-renewing human HSCs.

In all mice injected with Lin$^-$hCD34$^+$hCD38$^-$ cells, hGPA$^+$ erythroid cells and hCD41a$^+$ megakaryocytes were present (not shown). We then tested whether differentiation of Lin$^-$hCD34$^+$hCD38$^-$ HSCs in the NOD/SCID/IL2rγ$^{null}$ mouse microenvironment can recapitulate normal developmental processes in the human bone marrow. We and others have reported that phenotypically separable myeloid and lymphoid progenitors are present in the steady-state normal bone marrow in both mice[38,39] and humans.[28,29] Figure 2C shows the representative FACS analysis data of recipient's bone marrow cells. In all 3 mice tested, the bone marrow contained the hCD34$^+$hCD38$^-$ HSC[36,37] and the hCD34$^+$hCD38$^+$ progenitor fractions.[28] The hCD34$^+$hCD38$^+$hCD10$^+$hCD127 (IL-7Rα)$^+$ common lymphoid progenitor (CLP) population[29] was detected (Figure 2C, top panels). According to the phenotypic definition of human myeloid progenitors,[28] the hCD34$^+$hCD38$^+$ progenitor fraction was subfractionated into hCD45RA$^-$hCD123 (IL-3Rα)$^{lo}$ common myeloid progenitor (CMP), hCD45RA$^-$hCD123$^-$ megakaryocyte/erythrocyte progenitor (MEP), and hCD45RA$^+$hCD123$^{lo}$ granulocyte/monocyte progenitor (GMP) populations (Figure 2C, bottom panels). We then purified these myeloid progenitors, and tested their differentiation potential. As shown in Figure 2D, purified GMPs and MEPs generated granulocyte/monocyte (GM)– and megakaryocyte/erythrocyte (MegE)–related colonies, respectively, while CMPs as well as HSCs generated mixed colonies in addition to GM and MegE colonies. These data strongly suggest that hCD34$^+$hCD38$^-$ human HSCs differentiate into all myeloid and lymphoid lineages tracking normal developmental steps of the steady-state human hematopoiesis within the NOD/SCID/IL2rγ$^{null}$ mouse bone marrow.

### Development of human systemic and mucosal immune systems in NOD/SCID/IL2rγ$^{null}$ mice

We further evaluated development of the human immune system in NOD/SCID/IL2rγ$^{null}$ recipients. In the thymus, thymocytes were mostly consisted of hCD3$^+$ T cells with scattered hCD19$^+$ B cells (Figure 3A-B). This is reasonable since the normal murine thymus contain a small number of B cells in addition to T cells.[40]

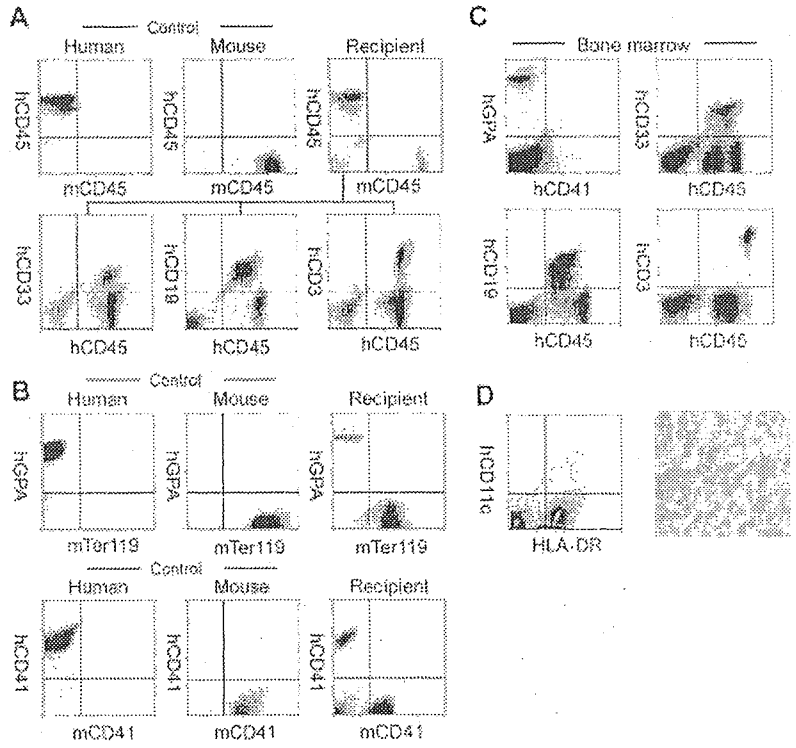


**Figure 1. Analysis of human hematopoietic cells in NOD/SCID/IL2rγ$^{null}$ recipients.** (A) In the scatter gates for nucleated cells, anti-hCD45 and anti-mCD45 antibodies (Abs) reacted exclusively with human and murine leukocytes, respectively. In the recipient blood, the majority of nucleated cells were human leukocytes (top row). High levels of engraftment by hCD33$^+$ myelomonocytic cells, hCD19$^+$ B cells, and hCD3$^+$ T cells were achieved in peripheral blood of recipient mice given transplants of Lin$^-$hCD34$^+$ CB cells (bottom row). (B) Analysis of circulating erythrocytes (top row) or platelets (bottom row) in a NOD/SCID/IL2rγ$^{null}$ recipient. In the blood, Ter119$^+$ murine erythrocytes as well as hGPA$^+$ human erythrocytes were detected. mCD41a$^+$ murine platelets were also reconstituted. (C) Multilineage engraftment of human cells in the NOD/SCID/IL2rγ$^{null}$ murine bone marrow. hCD33$^+$ myelomonocytic cells, hCD19$^+$ B cells, and hCD3$^+$ T cells were present. hGPA$^+$ erythroid cells and hCD41a$^+$ megakaryocytes were also seen in the nucleated cell gate of the bone marrow. (D, left) HLA-DR$^+$hCD11c$^+$ dendritic cells were detected in the spleen by a flow cytometric analysis. (Right) Immunohistochemical staining of CD11c in the spleen. CD11c$^+$ cells displayed dendritic cell morphology.

Thymocytes consisted of immature hCD4$^+$hCD8$^+$ double-positive (DP) T cells (Figure 3C) as well as small numbers of hCD4$^+$ or hCD8$^+$ single-positive (SP) mature T cells (Figure 4A, top panel), while hCD3$^+$ human T cells in spleen were mainly constituted of either hCD4$^+$ or hCD8$^+$ single positive T cells (Figure 4A, bottom panel). These data suggest that normal selection processes of T-cell development may occur in the recipients' thymi.

In the spleen, lymphoid follicle-like structures were seen (Figure 3D-E), where predominant hCD19$^+$ B cells were associated with surrounding scattered hCD3$^+$ T cells (Figure 3F). Development of mesenteric lymph nodes was also observed, where the similar follicle-like structures consisted of human B and T cells were present (not shown). In the bone marrow and the spleen, nucleated cells in each organ contained hCD34$^+$hCD19$^+$ pro-B cells, hCD10$^+$hCD19$^+$ immature B cells, and hCD19$^-$hCD20$^+$ mature B cells (Figure 4B). Figure 4C shows the expression of human immunoglobulins on hCD19$^+$ B cells. A significant fraction of hCD19$^+$ B cells expressed human IgM on their surface. A

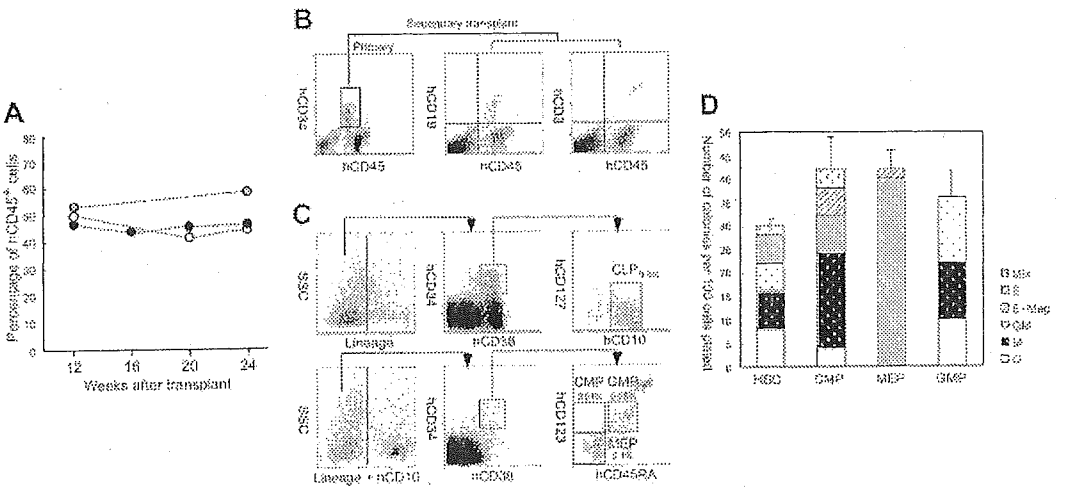


**Figure 2. Purified Lin$^-$hCD34$^+$hCD38$^-$ CB cells reconstitute hematopoiesis via physiological intermediates, and display long-term reconstitution in the NOD/SCID/IL2rγ$^{null}$ newborn system.** (A) Serial evaluation of chimerism of human cells in peripheral blood of recipient mice injected with 2 × 10$^4$ Lin$^-$hCD34$^+$hCD38$^-$ CB cells. White, gray, and black dots represent 3 individual recipients. (B) hCD34$^+$ cells purified from a primary recipient marrow (left) were successfully engrafted into the secondary newborn recipients. hCD19$^+$ B cells (middle) and hCD3$^+$ T cells (right) in a representative secondary recipient is shown. (C) The Lin$^-$ bone marrow cells contained hCD34$^+$hCD38$^-$hCD10$^+$hCD127 (IL-7Rα)$^+$ CLPs (top row). In the Lin$^-$hCD10$^-$fraction, hCD34$^+$hCD38$^+$hCD45RA$^-$hCD123 (IL-3Rα)$^{lo}$ CMPs, hCD34$^+$hCD38$^+$hCD45RA$^+$hCD123$^{lo}$ GMPs, hCD34$^+$hCD38$^+$hCD45RA$^-$hCD123$^-$ MEPs were present. Each number for progenitors indicates percentages of hCD45$^+$ cells. SSC indicates side scatter. (D) Colony-forming activity of purified myeloid progenitor population in the methylcellulose assay. Representative data from 1 of 3 recipients are shown. Error bars represent standard deviation.

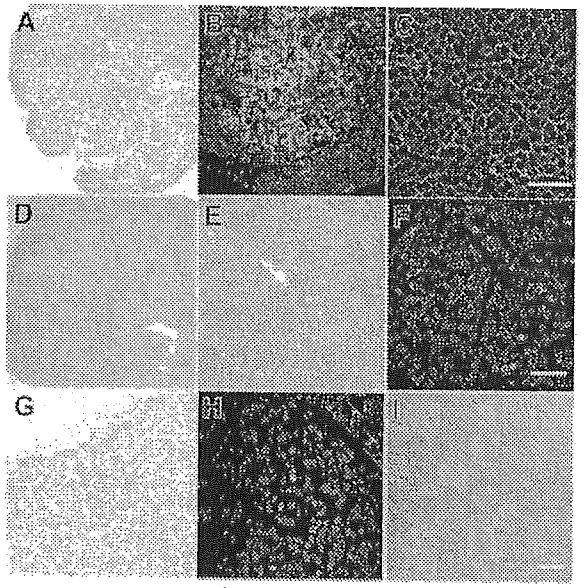


**Figure 3. Histology of lymphoid organs in engrafted NOD/SCID/IL2rγ$^{null}$ recipients.** (A) The thymus showed an increased cellularity after reconstitution. (B) The thymus stained with anti-hCD3 (green) and anti-hCD19 (red) antibodies. (C) The thymus stained with anti-hCD4 (green) and anti-hCD8 (red) antibodies. The majority of thymocytes are doubly positive for hCD4 and hCD8. (D-E) Lymphoid follicle-like structures in the spleen of a recipient. (F) The lymphoid follicles mainly contained hCD19$^+$ B cells (red) that were surrounded by scattered hCD3$^+$ T cells (green). (G) Histology of the intestine in an engrafted NOD/SCID/IL2rγ$^{null}$ recipient (left). (H) In the intestine, DAPI$^+$ (4′,6-diamidino-2-phenylindole)–nucleated cells (blue) contained both scattered hCD3$^+$ T cells (green) and human IgA$^+$ cells (red). (I) The DIC image of the same section shows that IgA$^+$ B cells were mainly found in the interstitial region of the intestinal mucosal layer. White bars inside panels represent 80 μm (C), 100 μm (F), and 20 μm (I).

fraction of cells expressing IgD were also observed in the blood and the spleen, suggesting that class switching occurred in these developing B cells. As reported in the Rag2$^{-/-}$ γc$^{-/-}$ mouse models,[10,12,14] hCD19$^+$IgA$^+$ B cells were detected in the bone marrow and the spleen in NOD/SCID/IL2rγ$^{null}$ recipients. We then evaluated concentrations of human immunoglobulins in sera of mice given transplants of human Lin$^-$hCD34$^+$ CB cells by ELISA. In all sera from 3 NOD/SCID/IL2rγ$^{null}$ recipients, a significant amount of IgG (257 ± 76 μg/mL) and IgM (600 ± 197 μg/mL) were detectable, whereas sera from the control NOD/SCID/β2m$^{-/-}$ mice contained lower levels of IgM (76 ± 41 μg/mL) and little or no IgG (Table S1, available on the *Blood* website; see the Supplemental Table link at the top of the online article). These data collectively suggest that class-switching can effectively occur in NOD/SCID/IL2rγ$^{null}$ mice.

The intestinal tract is one of the major sites for supporting host defense against exogenous antigens. Since bone marrow and spleen hCD19$^+$ B cells contained a significant fraction of cells expressing IgA, we tested whether reconstitution of mucosal immunity could be achieved in the NOD/SCID/IL2rγ$^{null}$ recipients. Immunohistologic analyses demonstrated that the intestinal tract of recipient mice contained significant numbers of cells expressing human IgA in addition to hCD3$^-$ T cells (Figure 3G-I). Thus, human CB cells could reconstitute cells responsible for both systemic and mucosal immunity in the NOD/SCID/IL2rγ$^{null}$ newborn system.

### Function of adaptive human immunity in engrafted NOD/SCID/IL2rγ$^{null}$ mice

Five NOD/SCID/IL2rγ$^{null}$ mice reconstituted with 3 independent human CB samples were immunized twice with ovalbumin (OVA) at 3 months after transplantation. Two weeks after immunization, sera were collected from these immunized mice, and were subjected to ELISA to quantify OVA-specific human IgG and IgM. As shown in Figure 5A, significant levels of OVA-specific human IgM and IgG were detected in all serum samples from immunized mice, but not in samples from nonimmunized engrafted mice. Thus, the adaptive human immune system properly functioned in the NOD/SCID/IL2rγ$^{null}$ strain to produce antigen-specific human IgM and IgG antibodies.

We next tested the alloantigen-specific cytotoxic function of human T cells developed in NOD/SCID/IL2rγ$^{null}$ recipients. hCD3$^+$ T cells isolated from the spleen of NOD/SCID/IL2rγ$^{null}$ recipients were cultured with allogeneic B-LCL (TAK-LCL). We established 8 hCD4$^+$ and 10 hCD8$^+$ T-cell clones responding LCL-specific allogeneic antigens. We then estimated cytotoxic activity of these T-cell clones in the presence or absence of anti–HLA-DR and anti–HLA class I antibodies. We randomly chose 3 each of CD4 and CD8 clones for further analysis (Figure 5B). A $^{51}$Cr release assay revealed that both hCD4$^+$ and hCD8$^+$ T cell clones exhibited cytotoxic activity against allogeneic TAK-LCL, whereas they showed no cytotoxicity against KIN-LCL, a cell line not sharing HLA classes I or II with TAK-LCL. Cytotoxic activity of hCD4$^+$

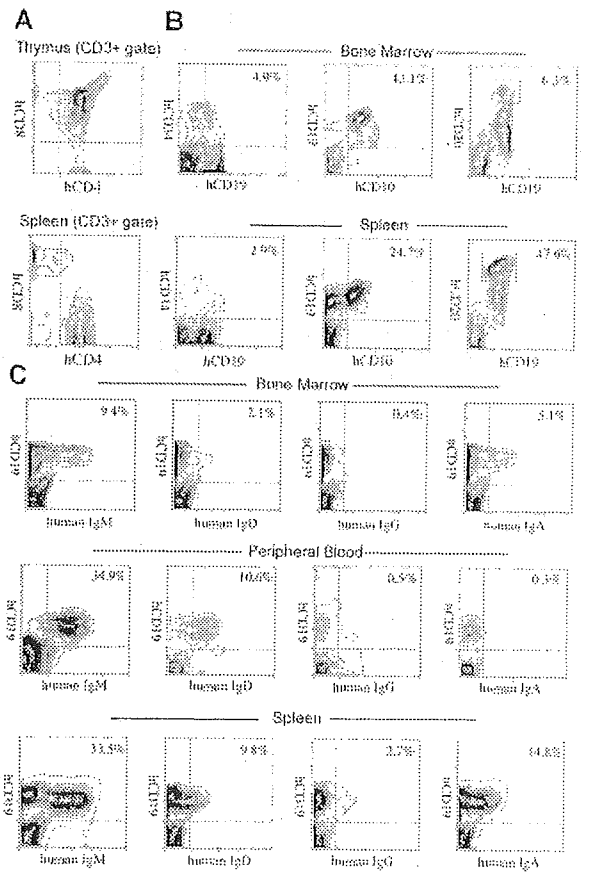


**Figure 4. Development of lymphocytes in NOD/SCID/IL2rγ$^{null}$ recipients.** (A) The flow cytometric analysis of human T cells in recipients. The majority of cells in the thymus were hCD4$^+$hCD8$^-$ double-positive thymocytes (top). The CD3$^+$ spleen cells contained hCD4$^+$ or hCD8$^+$ single-positive mature T cells (bottom). (B) hCD34$^+$hCD19$^+$ pro-B, hCD10$^+$hCD19$^+$ pre-B, and hCD19$^+$hCD20$^{hi}$ mature B cells were seen in different proportions in the bone marrow and the spleen of recipient mice. Numbers represent percentages within total nucleated cells. (C) B cells expressing each class of human immunoglobulin heavy chain were seen in the bone marrow, the peripheral blood (PB), or the spleen of engrafted NOD/SCID/IL2rγ$^{null}$ mice. Numbers represent percentages out of nucleated cells.

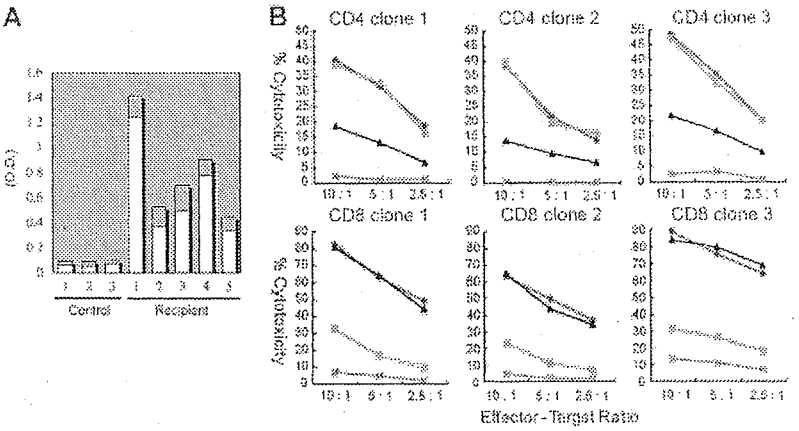


**Figure 5. Functional analysis of human T and B cells developed in NOD/SCID/IL2rγ$^{null}$ recipients.** (A) Production of OVA-specific human immunoglobulins. Two weeks after immunization with OVA, sera of 5 independent recipients were sampled, and were evaluated for the concentration of OVA-specific human IgM (□) and IgG (▩) by ELISA. Sera of 3 nonimmunized NOD/SCID/IL2rγ$^{null}$ recipients were used as controls. O.D. indicates optical density. (B) Cytotoxic activity of human T cells generated in NOD/SCID/IL2rg-null mice. hCD4$^+$ and hCD8$^+$ T-cell clones derived from the recipient spleen were cocultured with allogeneic target cells (TAK-LCLs). KIN-LCLs that do not share any HLA type with effector cells or TAK-LCLs (X) were used as negative controls. Both hCD4$^+$ and hCD8$^+$ T-cell lines displayed cytotoxic activity against TAK-LCL in a dose-dependent manner. In hCD4$^+$ T-cell clones, this effect was blocked by anti–HLA-DR antibodies (▲), whereas in hCD8$^+$ T-cell clones, the effect was blocked by anti–HLA class I antibodies (▩). ♦ indicates cytotoxic response to TAK-LCLs without addition of antibodies.

and hCD8$^+$ T cell clones was significantly inhibited by the addition of anti–HLA-DR and anti–HLA class I antibodies, respectively. These data clearly demonstrate that human CB-derived T cells can exhibit cytotoxic activity in an HLA-restricted manner.

## Discussion

Xenogeneic transplantation models have been extensively used to study human hematopoiesis in vivo.[1,41,42] In the present study, we describe a new xenogeneic transplantation system that effectively supports human hemato-lymphoid development of all lineages for the long term.

NOD/SCID/IL2rγ$^{null}$ newborns exhibited very efficient reconstitution of human hematopoietic and immune systems after intravenous injection of a relatively small number of CB cells. In our hands, NOD/SCID/IL2rγ$^{null}$ newborns displayed a significantly higher chimerism of human blood cells compared with NOD/SCID/β2m$^{-/-}$ newborns under an identical transplantation setting (Table 1). This result directly shows that the IL2rγ$^{null}$ mutation has a merit on human cell engraftment over the β2m$^{-/-}$ mutation.

One of the critical problems in the NOD/SCID strain for the use of recipients is that this mouse line possesses a predisposition to thymic lymphoma due to an endogenous ectropic provirus (Emv-30).[32] Because of this, NOD/SCID and NOD/SCID/β2m$^{-/-}$ mice have the short mean lifespan of 8.5 and 6 months, respectively, while NOD/SCID/IL2rγ$^{null}$ mice did not develop thymic lymphoma surviving more than 15 months,[31] which allows a long-term experimentation.

In our study, NOD/SCID/IL2rγ$^{null}$ newborns injected with $10^5$ hCD34$^+$ CB cells via a facial vein consistently displayed high levels of chimerism of human hematopoiesis (50%-80%; Table 1). This model is comparable to, or may be more efficient than the Rag2$^{-/-}$ γc$^{-/-}$ newborn model where intrahepatic injection of 0.4 to 1.2 × $10^5$ hCD34$^+$ CB cells generated variable levels of chimerism of human cells (5%-65%).[14] This slight difference of engraftment efficiency, however, could reflect the homing efficiency of HSCs by each injection route. The NOD/SCID/IL2rγ$^{null}$ newborn model might be more efficient than the NOD/SCID/γc$^{-/-}$ adult model in which the majority of recipients showed approximately 30% chimerism of human cells after transplantation of 5 × $10^4$ hCD34$^+$ CB cells.[11] Although we did not test NOD/SCID/γc$^{-/-}$ newborns side by side in this study, we have found that the engraftment level of hCD34$^+$ cells of human acute myelogenous leukemia is approximately 3-fold higher in newborns than adults in the NOD/SCID/IL2rγ$^{null}$ strain (F.I., T.M., S.Y., M.Y., M.H., K.A., and L.D.S., manuscript in preparation). Therefore, it remains unclear whether the IL2rγ$^{null}$ mutation has a significant advantage over the truncated γc mutation[11] for human cell engraftment. It is still possible that the improved engraftment efficiencies in the NOD/SCID/IL2rγ$^{null}$ newborn system as compared to those in the NOD/SCID/γc$^{-/-}$ adult system reflect the age-dependent maturation of the xenogeneic barrier.

The Rag2$^{-/-}$ γc$^{-/-}$ newborn and NOD/SCID/γc$^{-/-}$ adult models have provided definitive evidences that functional T cells, B cells, and dendritic cells can develop from hematopoietic progenitor cells in immunodeficient mice. Class-switching of immunoglobulin in CB-derived B cells properly occurred in the NOD/SCID/IL2rγ$^{null}$ but not in the NOD/SCID/β2m$^{-/-}$ newborns (Table S1), further confirming the advantage of the NOD/SCID/IL2rγ$^{null}$ model. We also showed that, consistent with a previous report using the Rag2$^{-/-}$ γc$^{-/-}$ model,[14] human T and B cells developed in NOD/SCID/IL2rγ$^{null}$ mice are capable of mounting antigen-specific immune responses. Interestingly, human T and B cells migrated into murine lymphoid organs and into the intestinal tissues to collaborate in forming lymphoid organ structures. Furthermore, we found that IgA-secreting human B cells can develop in the murine intestine, suggesting that human mucosal immunity could be generated. Thus, the cellular interaction and the lymphocyte homing could occur at least to some extent across the xenogenic barrier in this model. It is also of interest that developing human cells in the thymus displayed normal distribution of SP and DP cells (Figure 4A), and that mature human T cells displayed cytotoxic functions in an HLA-dependent manner (Figure 5B). This suggests that positive and/or negative selection of human T cells could occur in NOD/SCID/IL2rγ$^{null}$ recipients. Thymic epithelial cells in recipients reacted with anti-murine but not anti-human centromere probes in a FISH assay (F.I. and M.H., unpublished data, September 2004), confirming their recipient's origin. Thus, it remains unclear how these human T cells effectively educated and developed in murine thymus. It is also possible that human mature T cells developed by extrathymic education and selection.

Our data directly show that the most primitive hCD34$^+$hCD38$^-$ CB cells are capable of generating the human myeloerythroid system in addition to the immune system in the NOD/SCID/IL2rγ$^{null}$ recipients. The emergence of circulating hCD33$^+$ myelomonocytic cells after transplantation of human CB cells has been reported in the NOD/SCID/β2m$^{-/-}$ newborn[33] and the NOD/SCID/γc$^{-/-}$ adult[11] systems. Development of human erythropoiesis, however, has not been obtained in previous models,

although it has been reported that NOD/SCID mice can support terminal maturation of hCD71$^+$ erythroblasts that were induced ex vivo from human HSCs by culturing with human cytokines.[43] We showed for the first time that human erythropoiesis and thrombopoiesis can develop in mice from primitive hCD34$^-$hCD38$^-$ cells, as evidenced by the presence of erythroblasts and megakaryocytes in the bone marrow and of circulating erythrocytes and platelets in NOD/SCID/IL2r$\gamma^{null}$ recipients. It is important to note that the hCD34$^+$hCD38$^-$ CB HSC population generated myeloid- and lymphoid-restricted progenitor populations such as CMPs, GMPs, MEPs, and CLPs in the bone marrow (Figure 2E-F). Thus, the NOD/SCID/IL2r$\gamma^{null}$ microenvironment might be able to support physiological steps of myelopoiesis and lymphopoiesis initiating from the primitive HSC stage.

In summary, we show that the NOD/SCID/IL2r$\gamma^{null}$ newborn system efficiently supports hemato-lymphoid development from primitive human HSCs, passing through physiological developmental intermediates. It also can support development of human systemic and mucosal immunity, and therefore may be useful to use human immunity to produce immunoglobulins or experimental vaccines. The NOD/SCID/IL2r$\gamma^{null}$ newborn system might also serve as an efficient tool for understanding malignant hematopoiesis in humans, since the analysis of human leukemogenesis has mainly been dependent upon the NOD/SCID adult mouse system.[44-46] Our model might also be useful to reproduce the transforming process of human hematopoietic cells, as transplanted murine hematopoietic progenitor and stem cells can develop leukemia by transducing oncogenic fusion genes in syngeneic mouse models.[47,48] Thus, the use of this system should open a more efficient way to analyze normal and malignant human hematopoiesis.

## Acknowledgments

We thank Bruce Gott and Lisa Burzenski for excellent technical assistance, and Dr Sato and other staff at Fukuoka Cord Blood Bank for preparation of CB.

## References


1. Greiner DL, Hesselton RA, Shultz LD. SCID mouse models of human stem cell engraftment. Stem Cells. 1998;16:166-177.
2. McCune JM, Namikawa R, Kaneshima H, Shultz LD, Lieberman M, Weissman IL. The SCID-hu mouse: murine model for the analysis of human hematolymphoid differentiation and function. Science. 1988;241:1632-1639.
3. Mosier DE, Gulizia RJ, Baird SM, Wilson DB. Transfer of a functional human immune system to mice with severe combined immunodeficiency. Nature. 1988;335:256-259.
4. Kaneshima H, Namikawa R, McCune JM. Human hematolymphoid cells in SCID mice. Curr Opin Immunol. 1994;6:327-333.
5. Pflumio F, Izac B, Katz A, Shultz LD, Vainchenker W, Coulombel L. Phenotype and function of human hematopoietic cells engrafting immune-deficient CB17-severe combined immunodeficiency mice and nonobese diabetic-severe combined immunodeficiency mice after transplantation of human cord blood mononuclear cells. Blood. 1996;88:3731-3740.
6. Shultz LD, Lang PA, Christianson SW, et al. NOD/LtSz-Rag1null mice: an immunodeficient and radioresistant model for engraftment of human hematolymphoid cells, HIV infection, and adoptive transfer of NOD mouse diabetogenic T cells. J Immunol. 2000;164:2496-2507.
7. Goldman JP, Blundell MP, Lopes L, Kinnon C, Di Santo JP, Thrasher AJ. Enhanced human cell engraftment in mice deficient in RAG2 and the common cytokine receptor gamma chain. Br J Haematol. 1998;103:335-342.
8. Greiner DL, Shultz LD, Yates J, et al. Improved engraftment of human spleen cells in NOD/LtSz-scid/scid mice as compared with C.B-17-scid/scid mice. Am J Pathol. 1995;146:888-902.
9. Yoshino H, Ueda T, Kawahata M, et al. Natural killer cell depletion by anti-asialo GM1 antiserum treatment enhances human hematopoietic stem cell engraftment in NOD/Shi-scid mice. Bone Marrow Transplant. 2000;26:1211-1216.
10. Kollet O, Peled A, Byk T, et al. beta2 microglobulin-deficient (B2m(null)) NOD/SCID mice are excellent recipients for studying human stem cell function. Blood. 2000;95:3102-3105.
11. Ito M, Hiramatsu H, Kobayashi K, et al. NOD/SCID/gamma(c)(null) mouse: an excellent recipient mouse model for engraftment of human cells. Blood. 2002;100:3175-3182.
12. Hiramatsu H, Nishikomori R, Heike T, et al. Complete reconstitution of human lymphocytes from cord blood CD34+ cells using the NOD/SCID/gammacnull mice model. Blood. 2003;102:873-880.
13. Leonard WJ. Cytokines and immunodeficiency diseases. Nat Rev Immunol. 2001;1:200-208.
14. Traggiai E, Chicha L, Mazzucchelli L, et al. Development of a human adaptive immune system in cord blood cell-transplanted mice. Science. 2004; 304:104-107.
15. Ohbo K, Suda T, Hashiyama M, et al. Modulation of hematopoiesis in mice with a truncated mutant of the interleukin-2 receptor gamma chain. Blood. 1996;87:956-967.
16. Cao X, Shores EW, Hu-Li J, et al. Defective lymphoid development in mice lacking expression of the common cytokine receptor gamma chain. Immunity. 1995;2:223-238.
17. DiSanto JP, Muller W, Guy-Grand D, Fischer A, Rajewsky K. Lymphoid development in mice with a targeted deletion of the interleukin 2 receptor gamma chain. Proc Natl Acad Sci U S A. 1995; 92:377-381.
18. Asao H, Takeshita T, Ishii N, Kumaki S, Nakamura M, Sugamura K. Reconstitution of functional interleukin 2 receptor complexes on fibroblastoid cells: involvement of the cytoplasmic domain of the gamma chain in two distinct signaling pathways. Proc Natl Acad Sci U S A. 1993;90: 4127-4131.
19. Takeshita T, Asao H, Ohtani K, et al. Cloning of the gamma chain of the human IL-2 receptor. Science. 1992;257:379-382.
20. Russell SM, Keegan AD, Harada N, et al. Interleukin-2 receptor gamma chain: a functional component of the interleukin-4 receptor. Science. 1993;262:1880-1883.
21. Noguchi M, Nakamura Y, Russell SM, et al. Interleukin-2 receptor gamma chain: a functional component of the interleukin-7 receptor. Science. 1993;262:1877-1880.
22. Kondo M, Takeshita T, Higuchi M, et al. Functional participation of the IL-2 receptor gamma chain in IL-7 receptor complexes. Science. 1994; 263:1453-1454.
23. Kondo M, Takeshita T, Ishii N, et al. Sharing of the interleukin-2 (IL-2) receptor gamma chain between receptors for IL-2 and IL-4. Science. 1993; 262:1874-1877.
24. Ferrag F, Pezet A, Chiarenza A, et al. Homodimerization of IL-2 receptor beta chain is necessary and sufficient to activate Jak2 and downstream signaling pathways. FEBS Lett. 1998;421: 32-36.
25. Reichel M, Nelson BH, Greenberg PD, Rothman PB. The IL-4 receptor alpha-chain cytoplasmic domain is sufficient for activation of JAK-1 and STAT6 and the induction of IL-4-specific gene expression. J Immunol. 1997;158:5860-5867.
26. Shultz LD, Lyons BL, Burzenski LM, et al. Human lymphoid and myeloid cell development in NOD/LtSz-scid IL2rgnull mice engrafted with mobilized human hematopoietic stem cells. J Immunol. 2005;174:6477-6489.
27. Sands MS, Barker JE, Vogler C, et al. Treatment of murine mucopolysaccharidosis type VII by syngeneic bone marrow transplantation in neonates. Lab Invest. 1993;68:676-686.
28. Manz MG, Miyamoto T, Akashi K, Weissman IL. Prospective isolation of human clonogenic common myeloid progenitors. Proc Natl Acad Sci U S A. 2002;99:11872-11877.
29. Galy A, Travis M, Cen D, Chen B. Human T, B, natural killer, and dendritic cells arise from a common bone marrow progenitor cell subset. Immunity. 1995;3:459-473.
30. LeBien TW. Fates of human B-cell precursors. Blood. 2000;96:9-23.
31. Yanai F, Ishii E, Kojima K, et al. Essential roles of perforin in antigen-specific cytotoxicity mediated by human CD4+ T lymphocytes: analysis using the combination of hereditary perforin-deficient effector cells and Fas-deficient target cells. J Immunol. 2003;170:2205-2213.
32. Prochazka M, Gaskins HR, Shultz LD, Leiter EH. The nonobese diabetic scid mouse: model for spontaneous thymomagenesis associated with immunodeficiency. Proc Natl Acad Sci U S A. 1992;89:3290-3294.
33. Ishikawa F, Livingston AG, Wingard JR, Nishikawa S, Ogawa M. An assay for long-term engrafting human hematopoietic cells based on newborn NOD/SCID/beta2-microglobulin(null) mice. Exp Hematol. 2002;30:488-494.
34. Kina T, Ikuta K, Takayama E, et al. The monoclonal antibody TER-119 recognizes a molecule associated with glycophorin A and specifically marks the late stages of murine erythroid lineage. Br J Haematol. 2000;109:280-287.
35. Okuno Y, Iwasaki H, Huettner CS, et al. Differential regulation of the human and murine CD34 genes in hematopoietic stem cells. Proc Natl Acad Sci U S A. 2002;99:6246-6251.
36. Craig W, Kay R, Cutler RL, Lansdorp PM. Expression of Thy-1 on human hematopoietic progenitor cells. J Exp Med. Vol. 177; 1993:1331-1342.
37. Terstappen LW, Huang S, Safford M, Lansdorp

PM, Loken MR. Sequential generations of hematopoietic colonies derived from single nonlineage-committed CD34+CD38- progenitor cells. Blood. 1991;77:1218-1227.

38. Akashi K, Traver D, Miyamoto T, Weissman IL. A clonogenic common myeloid progenitor that gives rise to all myeloid lineages. Nature. 2000;404:193-197.
39. Kondo M, Weissman IL, Akashi K. Identification of clonogenic common lymphoid progenitors in mouse bone marrow. Cell. 1997;91:661-672.
40. Akashi K, Richie LI, Miyamoto T, Carr WH, Weissman IL. B lymphopoiesis in the thymus. J Immunol. 2000;164:5221-5226.
41. Zanjani ED. The human sheep xenograft model for the study of the in vivo potential of human HSC and in utero gene transfer. Stem Cells. 2000;18:151.
42. Stier S, Cheng T, Forkert R, et al. Ex vivo targeting of p21Cip1/Waf1 permits relative expansion of human hematopoietic stem cells. Blood. 2003;102:1260-1266.
43. Neildez-Nguyen TM, Wajcman H, Marden MC, et al. Human erythroid cells produced ex vivo at large scale differentiate into red blood cells in vivo. Nat Biotechnol. 2002;20:467-472.
44. Lumkul R, Gorin NC, Malehorn MT, et al. Human AML cells in NOD/SCID mice: engraftment potential and gene expression. Leukemia. 2002;16:1818-1826.
45. Hope KJ, Jin L, Dick JE. Acute myeloid leukemia originates from a hierarchy of leukemic stem cell classes that differ in self-renewal capacity. Nat Immunol. 2004;5:738-743.
46. Bonnet D, Dick JE. Human acute myeloid leukemia is organized as a hierarchy that originates from a primitive hematopoietic cell. Nat Med. 1997;3:730-737.
47. Cozzio A, Passegue E, Ayton PM, Karsunky H, Cleary ML, Weissman IL. Similar MLL-associated leukemias arising from self-renewing stem cells and short-lived myeloid progenitors. Genes Dev. 2003;17:3029-3035.
48. Huntly BJ, Shigematsu H, Deguchi K, et al. MOZ-TIF2, but not BCR-ABL, confers properties of leukemic stem cells to committed murine hematopoietic progenitors. Cancer Cell. 2004;6:587-596.

Available online at www.sciencedirect.com
SCIENCE DIRECT®
Leukemia Research 29 (2005) 761–769
Leukemia Research
www.elsevier.com/locate/leukres

# Transgenic mice overexpressing murine thrombopoietin develop myelofibrosis and osteosclerosis

Haruko Kakumitsu [a,b], Kenjirou Kamezaki [a,b], Kazuya Shimoda [a,b,*], Kennosuke Karube [c], Takashi Haro [a,b], Akihiko Numata [a,b], Koutarou Shide [a,b], Tadashi Matsuda [d], Kouichi Oshima [c], Mine Harada [a]

[a] *The First Department of Internal Medicine, Kyushu University Hospital, 3-1-1 Maidashi, Higashi-ku, Fukuoka, Fukuoka 812-8582, Japan*
[b] *Medicine and Biosystemic Science, Kyushu University Graduate School of Medical Sciences, 3-1-1 Maidashi, Higashi-ku, Fukuoka, Fukuoka 812-8582, Japan*
[c] *Department of Pathology, Fukuoka University, Fukuoka City, Japan*
[d] *Department of Immunology, Graduate School of Pharmaceutical Sciences, Hokkaido University, Kita-Ku Kita 12 Nishi 6, Sapporo 060-0812, Japan*

Received 11 August 2004; accepted 8 December 2004
Available online 2 March 2005

**Abstract**

Thrombopoietin (TPO) regulates megakaryocytopoiesis and platelet production in vivo and in vitro. Exogenous overexpression of TPO in vivo by viral-mediated gene transfer induced bone marrow (BM) fibrosis and osteosclerosis. On the other hand, transgenic mice (Tg) overexpressing TPO using a liver-specific apolipoprotein E (Apo-E) promoter did not exhibit myelofibrosis or osteosclerosis. These discrepancies in phenotype are not fully understood. Then we have investigated the consequences of long-term in vivo overexpression of TPO in a mouse model. Murine TPO Tg mice driven by the IgH promoter were generated. The number of platelets and neutrophils in peripheral blood, and the number of megakaryocytes and granulocytic immature cells in the BM was elevated, together with the number of progenitor cells for megakaryocyte and myeloid cells. TPO Tg mice demonstrated anemia but the number of progenitor cells for the erythrocyte was increased. TPO Tg mice developed myelofibrosis and osteosclerosis as they aged with extramedullary hematopoiesis in the spleen. As plasma transforming growth factors (TGF)-β1 and osteoprotegerin (OPG) levels were higher in TPO Tg mice than in wild-type mice, the development of myelofibrosis and osteosclerosis depends on local TPO levels in BM and might be due to elevated TGF-β1 and OPG.


*Keywords:* TPO; Myelofibrosis; c-mpl; OPG; TGF-β

## 1. Introduction

Thrombopoietin (TPO) is a hematopoietic growth factor that regulates megakaryocytopoiesis and platelet production in vivo and in vitro [1–3]. The liver and kidneys are the major sites for TPO production [4,5], although small amounts of TPO mRNA can be detected in a variety of organs and tissues. Administration of recombinant TPO results in elevated circulating platelet levels [2], and mutant mice deficient for TPO or TPO receptor show about an 80% reduction in platelet numbers [6,7], indicating that TPO is essential for megakaryocytopoiesis. TPO also has effects on hematopoietic stem cells and progenitor cells [8–12], although no substantial difference in the number of blood cells except for platelets was observed in either TPO or TPO receptor deficient mice. TPO promotes the growth of hematopoietic progenitor cells and augments the number of erythroid burst-forming units (BFU-E), granulocyte-macrophage colony forming units (CFU-GM), and mixed colony forming units (CFU-mix) in collaboration with early or late-acting cytokines [13].

Exogenous overexpression of TPO in vivo by viral-mediated gene transfer induced bone marrow (BM) fibrosis and osteosclerosis. These TPO-overexpressing mice were

* Corresponding author. Tel.: +81 92 642 5230; fax: +81 92 642 5247.
*E-mail address:* kshimoda@intmed1.med.kyushu-u.ac.jp (K. Shimoda).

0145-2126/$ – see front matter © 2005 Elsevier Ltd. All rights reserved.
doi:10.1016/j.leukres.2004.12.009